Copyright Warning & Restrictions

The copyright law of the United States (Title 17, United States Code) governs the making of photocopies or other reproductions of copyrighted material.

Under certain conditions specified in the law, libraries and archives are authorized to furnish a photocopy or other reproduction. One of these specified conditions is that the photocopy or reproduction is not to be "used for any purpose other than private study, scholarship, or research." If a, user makes a request for, or later uses, a photocopy or reproduction for purposes in excess of "fair use" that user may be liable for copyright infringement,

This institution reserves the right to refuse to accept a copying order if, in its judgment, fulfillment of the order would involve violation of copyright law.

Please Note: The author retains the copyright while the New Jersey Institute of Technology reserves the right to distribute this thesis or dissertation

Printing note: If you do not wish to print this page, then select "Pages from: first page # to: last page #" on the print dialog screen

ABSTRACT

GLASS TRANSITION TEMPERATURE OF PARTICLES FOR DRUG DELIVERY

by
Yiqing Yang

Drug delivery plays an important role in targeted therapies and nanoparticles which can be used as drug carriers and it's a frequently researched topic. Poly(lactic-co-glycolic acid) (PLGA), a highly biocompatible polymer, has been used as a drug delivery vehicle in many studies. One of the challenges facing drug delivery particles is the problem of burst release which is when a large amount of the drug is suddenly released from the particle once it is placed in the body. This is generally undesirable as usually a slow and controlled release is preferred. The glass transition temperature has an effect on drug release behavior like the burst effect. In the case of PLGA, the effect can be pronounced since the glass transition temperature is close to body temperature. The glass transition phenomena of PLGA has been well researched in the past but the effect of thermal history on glass transition temperature of PLGA is yet to be investigated. With the development of temperature modulated differential scanning calorimetry (DSC), however, the glass transition temperature can be well separated from the effects of polymer aging commonly seen overlapping the glass transition in the DSC scan on initial heating of polymer samples. Thus, temperature modulated DSC provides the possibility to study the effect of thermal history on glass transition temperature.

To accurately study the effects of thermal history on the glass transition temperature of PLGA particles, particles need to be made of the same size, using the same PLGA, by different methods. In this study, nanoprecipitation, nanoemulsion and electrospray jetting techniques are used to produce the PLGA nanoparticles. The size

is optimized for all three methods to provide the stable production of nanoparticles with similar size distributions. The size optimization includes determination of factors such as the optimal surfactant concentration, optimal polymer concentration, and optimal sonication time. Several sets of nanoparticles made from nanoprecipitation and nanoemulsion are tested using temperature modulated differential scanning calorimetry (TMDSC). Results show that a clear glass transition temperature can be measured on the first heating scan. From these preliminary samples, it appears as though nanoemulsion particles would be preferable over nanoprecipitation particles for drug delivery because for nanoemulsion samples the glass transition temperature is higher and closer to the bulk value and the transition happens over a smaller temperature range. This suggests that particles made by nanoemulsion would have less burst release than particles made by nanoprecipitation.

GLASS TRANSITION TEMPERATURE OF PARTICLES FOR DRUG DELIVERY

by
Yiqing Yang

A Thesis
Submitted to the Faculty of
New Jersey Institute of Technology
in Partial Fulfillment of the Requirements for the Degree of
Master of Science in Chemical Engineering

Otto H. York Department of
Chemical and Materials Engineering

May 2019

APPROVAL PAGE

GLASS TRANSITION TEMPERATURE OF PARTICLES FOR DRUG DELIVERY

Yiqing Yang

Dr. Kathleen McEnnis, Dissertation Advisor Assistant Professor of Chemical and Materials Engineering, NJIT	Date
Dr. Murat Guvendiren, Committee Member Assistant Professor of Chemical and Materials Engineering, NJIT	Date
Dr. Xiaoyang Xu, Committee Member Assistant Professor of Chemical and Materials Engineering, NJIT	Date

BIOGRAPHICAL SKETCH

Author: Yiqing Yang

Degree: Master of Science

Date: May 2019

Undergraduate and Graduate Education:

- Bachelor of Science in Chemistry,
  Anhui University, Anhui, P. R. China, 2016

Major: Chemical Engineering

This thesis is dedicated to my beloved parents for their full support.

Sen Yang

Huixian Ding

ACKNOWLEDGMENT

Thanks for the help of Dr. Kethleen McEnnis on research direction and polish of thesis. She provided the funds and important apparatus for the research which is crucial for getting this done. Without her help, the research cannot proceed. Thanks for the help on Dr. Murat Guvendiren and Dr. Xiaolong Xu for their support as committee member and their useful suggestions. Thanks for Qingrui Jiang and Steven Herrera's help on doing the experiments. Without their help, the experiments would get slowed down a lot. Thanks to my parents who provide their full support on me. Without them, I cannot finish my degree.

TABLE OF CONTENTS

TABLE OF CONTENTS
(Continued)

Chapter **Page**

TABLE OF CONTENTS
(Continued)

LIST OF TABLES

LIST OF FIGURES

LIST OF FIGURES
(Continued)

LIST OF FIGURES
(Continued)

CHAPTER 1

BACKGROUND INTRODUCTION

1.1 Nanoparticles, Drug Delivery and Glass Transition

PLGA nanoparticles are widely used for drug delivery [1,2]. PLGA is known for its biocompatibility and non-toxicity to cells. [3] PLGA has been extensively researched as a drug carrier for many applications such as dialysis, targeted therapy studies, cardiac myocytes, cancer, and many other applications. [4,5,6,7,8,9,11] PLGA can also be used as protein and DNA carriers [5,10] and it can also be applied in food and agricultural industries.[12]

It was investigated that PLGA's drug release behavior is affected by the glass transition temperature. [13,14,15] When the temperature of PLGA is higher than the glass transition temperature (or Tg), more drugs are released during the burst effect, which is a phenomena occurred shortly after the start of drug release where a significant amount of drugs get released within a short time. That is because when the temperature is above Tg, the PLGA transforms from a glassy solid into a soft rubbery material and in the meanwhile, more drug loaded inside PLGA will get suddenly released due to this transition. The long-term drug release is based on PLGA's biodegradation. It is also indicated that the closer Tg is to body temperature, the worse long-term drug release will be. [16,17]

The glass transition temperature of PLGA is well researched under the thermal history erased condition. [16,17] However, little is mentioned in the literature about the glass transition temperature of PLGA with different thermal history. In order to research the effect of thermal history on the glass transition temperature, three different methods, nanoprecipitation, nanoemulsion and electrospray, are used to produce three sets of

nanoparticles from the same PLGA with the same size but of different thermal history. To accomplish creating particles of the same size, all three different methods are required to be optimized.

1.2 Nanoemulsion

Nanoemulsion is a method used to produce nanoparticles. High energy sonication is one of the commonly used methods for nanoemulsion.[18] Below is an example image:

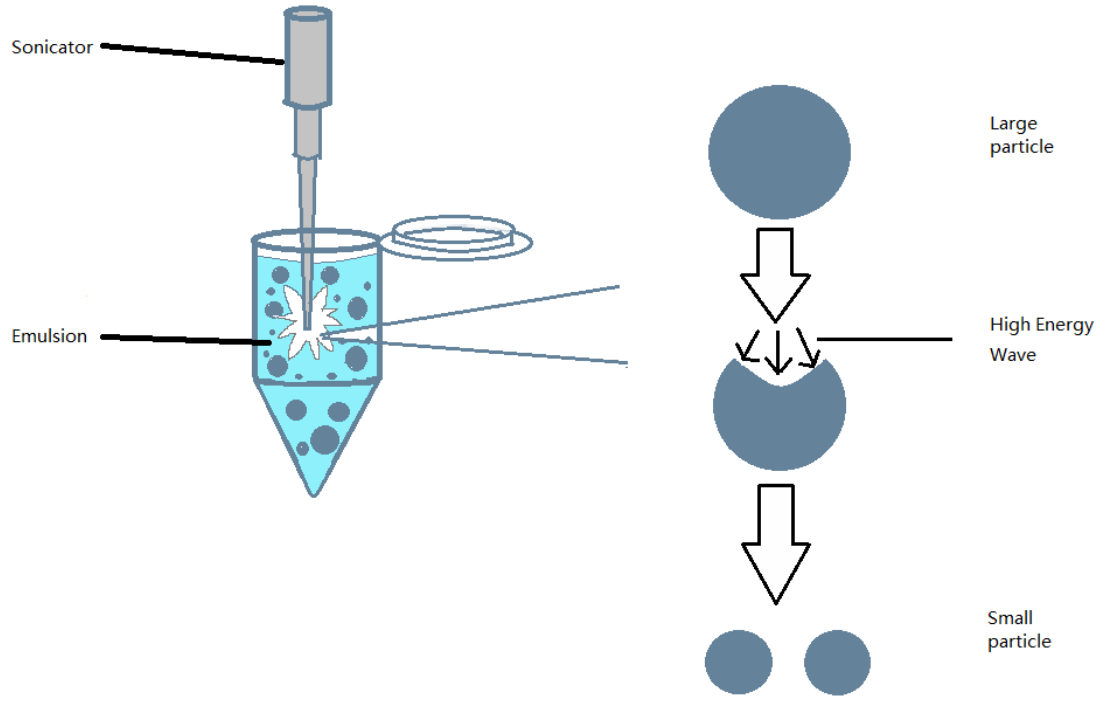

Figure 1.1 Example of high energy sonication nanoemulsion.

There are several types of nanoemulsion using ultrasonication for different conditions with specific order such as oil/water or water/oil single emulsions and water/oil/water or oil/water/oil double emulsions. [2,9,28] For example, the oil-water emulsion means the organic phase was injected into the aqueous phase and the mixture was sonicated. The water-oil-water double emulsion means the aqueous phase was

injected into the organic phase, the mixture was sonicated, the aqueous phase was added again, and the sample was sonicated again. Each specific method has different advantages and disadvantages. [19,20] Choice of method is usually based on whether the drugs are hydrophobic or hydrophilic. If the drug is hydrophobic, then oil in water emulsion will be used. If the drug is hydrophilic, the water in oil phase will be applied. A surfactant (also called an emulsifier) is required to keep the nanoparticles stable and prevent aggregation. [21] For different types of emulsions, different types of surfactant are required. Usually, if the surfactant is more soluble in water than oil, the formed emulsion will be oil-in-water. Instead, if the surfactant is more soluble in oil than water, the formed emulsion will be water-in-oil. After a mixture of the organic phase and the aqueous phase is created, the solution will be emulsified with sonication. If it's a double emulsion method, then a second sonication is required after the first. After the sonication, the sample will be left for evaporation of the organic phase. Later the sample is centrifuged to get rid of the surfactant dissolved in the water, leaving only nanoparticles in the solution. The solution is frozen and lyophilized at low temperature to avoid possible aging and degradation.

The particle size is mainly determined by the diffusion coefficient of the organic phase droplets in water. Factors likes temperature, ionic strength, organic concentration, and stabilizer concentration which can change the diffusion rate, are able to change the particle size. [20, 23] High polarity solvent also allows the organic phase to diffuse faster into aqueous phase, which also leads to smaller particles. [39]

A typical oil in water emulsion involves the following steps. The mixture phase is sonicated and emulsified in an emulsifier-containing aqueous phase. Then, the organic solvent diffuses from the droplets into the aqueous phase. After this, the diffused solvent is removed by evaporation and the nanoparticles solidify. The high

energy shock wave from the sonication process creates turbulence that forces the larger droplets to break into smaller droplets. Further shock waves break large particles and further reduce the size.[18] Increasing sonication energy and time can make the particle size smaller until a certain limit is reached where the size can't be further decreased because the energy provided is not enough to break the bounds within polymer.

The size of particles produced by nanoemulsion varies significantly when using different methods. Usually, the particles produced by nanoemulsion are larger than particles prepared by nanoprecipitation. For this work, the method used is the organic-water nanoemulsion because it has relatively less factors to control making particle size tuning less complicated.

1.2.1 Nanoemulsion Size Tuning

The size of the resulting particles from a nanoemulsion can be tuned by varying the conditions. The sonication process in particular will have a significant effect on particle size. [23] For example, the sonication time and the amplitude will have an effect on particle size. By increasing both of them, the size of the produced particles will be decreased. Also, increasing both sonication time and amplitude tends to increase the uniformity of the particle size resulting in a narrower size distribution. The concentration of the organic phase and the surfactant concentration can have an effect on the size as well. Like with nanoprecipitation, the temperature also plays a role on particle size. Decreasing the temperature leads to a decrease of the diffusion rate of the organic phase making the particle larger. Also, the effect of molecular weight of the polymer used to produce the nanoparticles is very important. The smaller the molecular

weight is, the easier it will be to form smaller particles. Different types of organic solvent and different types of surfactant also change the particle size.

1.3 Nanoprecipitation

Nanoprecipitation is a method of creating nanoparticles using a mixture of an organic phase and an aqueous phase. The polymer and drugs are dissolved in the organic phase. Then the organic phase is injected into the aqueous phase under stirring to prevent aggregation. Just like nanoemulsion technology, a surfactant is dissolved in the aqueous phase as stabilizer. Once the organic phase is injected into aqueous phase, the procedure of nucleation, growth and aggregation happens in order and forms nanoparticles immediately. After evaporation of the organic phase, the aqueous phase will be centrifuged, frozen and lyophilized to get the nanoparticles. The particle size can also be modified by changing the diffusion coefficient of the organic phase in water [6,20,24]. The image below shows an example of the nanoprecipitation procedure:

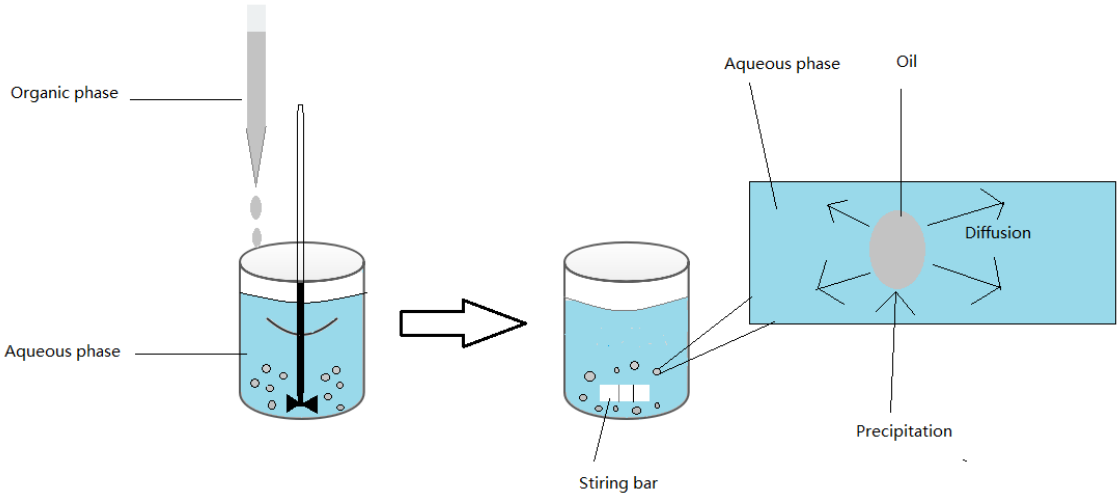

Figure 1.2 Example of nanoprecipitation.

The mechanism of nanoprecipitation includes 3 phases: nucleation, growth and aggregation. [12,18] The driving force of these three phases is the supersaturation of polymer in the solvent mixture. Below is an image of the mechanism of nanoprecipitation:

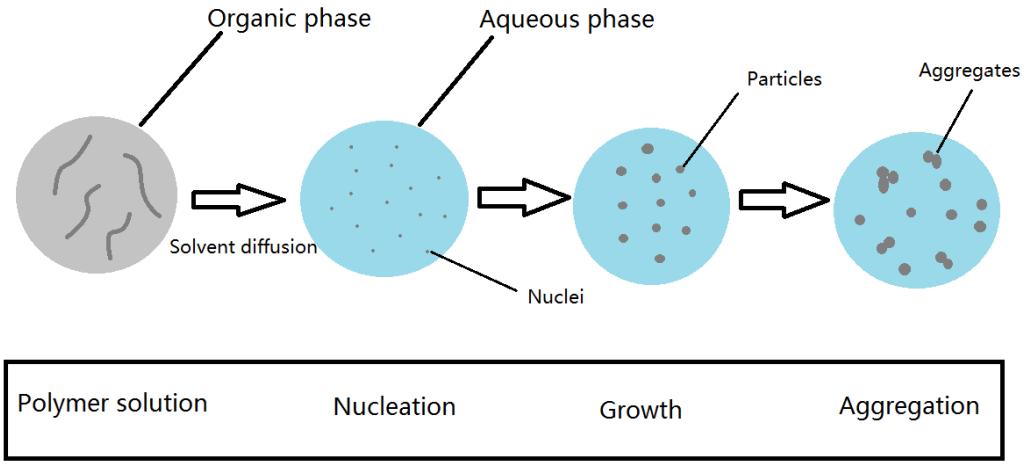

Figure 1.3 Mechanism of nanoprecipitation.

The supersaturation is usually defined as the ratio of actual polymer concentration (C_{pcl}) to solubility of the polymer ($C_{pcl.eq}$) in solvent mixture:

$$S = \frac{C_{pcl}}{C_{pcl.eq}}$$

Supersaturation determines the rate of nucleation. According to classical nucleation theory, the nucleation rate (J) can be calculated with the following equation:

$$J = \frac{2D}{d^5} \exp\left(-\frac{16\pi\gamma^3 v^2}{3{K_b}^3 T^3 [\ln(S)]^2}\right)$$

where k_b is the Boltzmann constant, T is the absolute temperature, D is the molecular diffusion of the polymer, d is the molecular diameter, γ is the interfacial tension of the formed particles with the solution, S is the supersaturation and υ is PLGA molecular volume. [25]

The growth is defined as the adhesion of polymer molecules diffused from the supersaturated solvent mixture to the surface of particles. The equation of the growth rate can be calculated by the following:

$$G = \frac{2K_m MCpcl}{\rho}(S-1)$$

where ρ is the density, K_m is the mass transfer coefficient, and M is the molecular weight of the polymer. [25]

The rate of aggregation is mainly affected by the collision frequency of polymer particles and their stability. The aggregation frequency which depends on the size of particles and the collision mechanism, can be calculated by the following equation when it's performed under constant diffusion coefficient of organic phase and the particles are nanosized, thus, Brownian motion becomes the predominant mechanism:

$$\beta(L,\lambda) = \frac{2K_b T}{3\mu}\frac{(L+\lambda)^2}{L\lambda}$$

L and λ are the size of the colliding particles, and μ is the viscosity of the suspending fluid. Because not all the collisions lead to aggregation, there is the existence of an efficiency parameter which ranges from 0 to 1 and directly applied to the equation (not displayed in the equation). [25] The efficiency parameter is used to describe the instability factor and the proportion of the colliding particles which stick together to form the aggregation. [25]

The whole process of nanoprecipitation is controlled by these speeds. The speed can be calculated from these equations and provides a mathematical way to predict and build models for mechanism study.

1.3.1 Nanoprecipitation Size Tuning

Tuning a nanoprecipitation recipe to create particles of a desired size can be very complicated as many factors can cause the size to change. For example, increasing organic phase concentration, increasing ionic strength of the solution, and increasing temperature can all increase the particle size. The size distribution can also be changed by centrifuging the sample to remove the unwanted sizes.

In sum, if anything changes the diffusion rate of the organic phase, it will lead to a change of the particle size and factors which don't change the diffusion rate won't change the particle size.[26]

Different types of organic solvent and surfactants also make the size different. Degradation effect is one of the effects which we want to avoid during the fabrication process. It can also cause the size to change and make the particles' properties and morphology different as well. The injection rate of organic phase doesn't have any effect on the particle size. Though research shows that surfactant is actually not necessary for producing nanoparticles, [27] surfactant is still necessary for when the organic solvent is immiscible with the aqueous phase while the surfactant free techniques need the organic solvent to be miscible.[28]

1.4 Electrospray Jetting

Electrospray is a method to create microparticles or nanoparticles with the use of a voltage source. The polymer dissolved in conductive organic solution is placed in a syringe. CTAB (Cetyl trimethylammonium bromide) is dissolved inside the organic solution together with polymer to increase the conductivity of the solution. The syringe is connected with a needle. The platform which is used to collect particles is grounded. Usually, a power supply is used to provide a stable voltage to the needle. The organic solution containing polymer is dripped to the bottom platform while the voltage is on. Very small droplets will start to fall to the bottom platform. The droplet is so small that the organic solvent will completely evaporate before the droplet reaches the bottom platform. And thus, only leave the particles on the bottom platform. Whether the created particles are nanoparticles or microparticles is dependent on the recipe used. [22] The image below shows how electrospray jetting works.

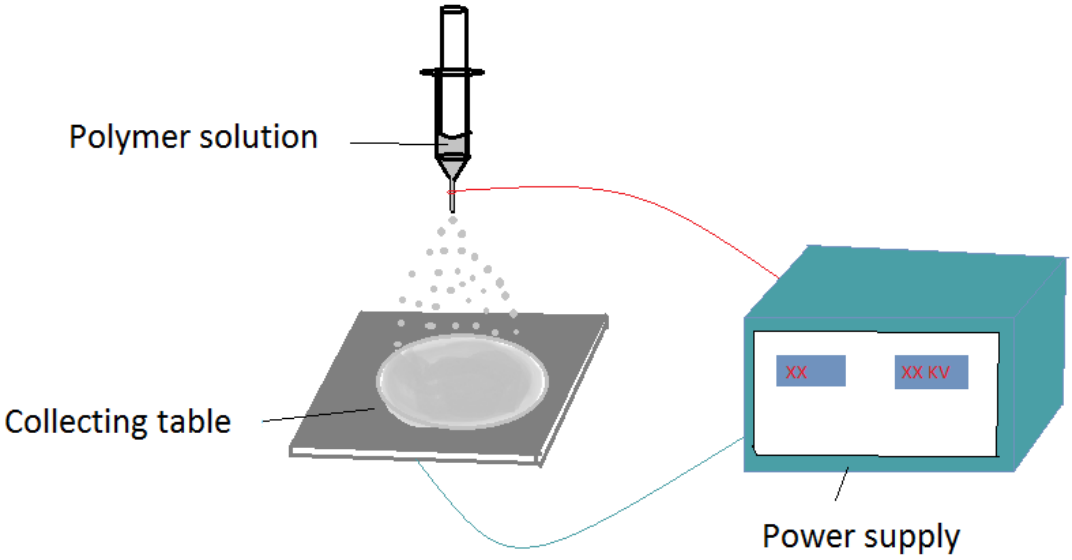

Figure 1.4 Example of electrospray jetting setting up.

1.4.1 Mechanism of Electrospray Jetting

The mechanism of electrospray jetting is to use the electrical field forces to overcome the surface tension of the droplet. When the droplet is formed at the end of needle, it will start to grow bigger due to the existence of surface tension. When the droplet is big enough, the gravity overcomes the surface tension and the big droplet starts to drop. When the electrical field is applied, the droplet becomes conductive due to the compounds dissolved inside the solution which increase the conductivity. The conductive droplet is under the effect of gravity, the electrical field force and the surface tension. The droplet will be a different shape under different electrical field forces. When the electrical field force can overcome the surface tension, a cone shape will be formed. This is called a Taylor cone.

At this point, the droplet will start to drop with a very limited weight. The droplet is so small that it is very hard to be observed by the eyes, but it can still be captured by a highspeed camera. Once the droplet is formed, the solvent will start to evaporate while falling down.

The solvent molecules will leave the droplet as neutral particles [30] and turned into lots of smaller droplets which will have its' solvent evaporate before the droplet can hit the collection plate, leaving behind only the very small particles to hit the collection plate. [31] Below is an example image.

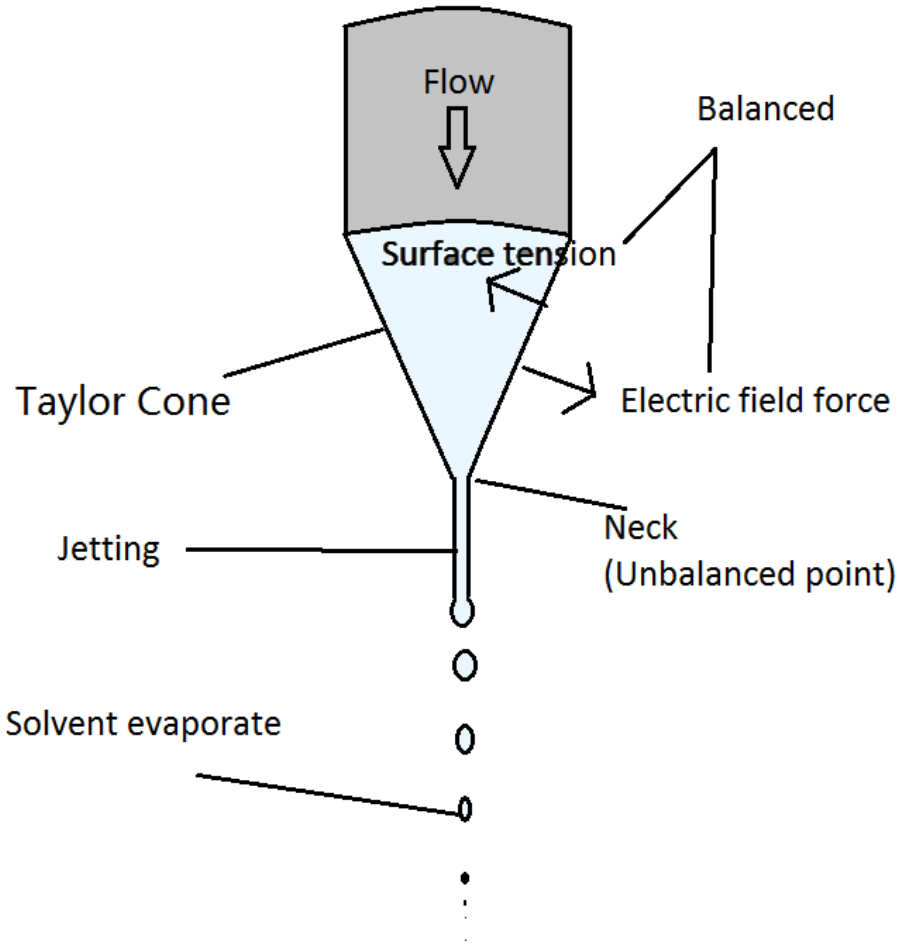

Figure 1.5 Mechanism of electrospray jetting.

1.4.2 Electrospray-Jetting Size Tuning

The size of particles made by electrospray-jetting can be tuned by adjusting the polymer concentration, polymer molecular weight, solvent ratio, and the addition of a charged salt. Generally, two different organic solvents are used, and the ratio of solvents will have a huge effect of the particle size. For example, when using the mixture of chloroform (Sigma-Aldrich catalog#:34854) and dimethylformamide (DMF) (Sigma-

Aldrich catalog#:270547) as the organic solvent, the increased ratio of chloroform to DMF can significantly increase the size uniformity and decrease the size. [30,32] However, this increased ratio also decreases the stability of the Taylor cone. Thus, choosing an appropriate recipe is an optimization between the stability and size. Increasing the concentration of the polymer also decreases the stability. While it increases the amount of PLGA jetted per minute, more PLGA will be wasted by forming large debris. Thus, jetting the same amount of PLGA with less amount of PLGA nanoparticles. Large molecular weight PLGA tends to increase the size of the particles and decreases the stability. Thus, the actual size tuning of particles made by electrospray jetting is a compromise between achieving the desired size and controlling the stability and productivity of the jet.

1.5 Degradation

The polymer we used is poly (lactic-co-glycolic acid), or PLGA. The properties of PLGA can be very different with different ratios of lactic acid to glycolic acid. With the increase in this ratio, the PLGA tends to be more durable and resistant to degradation. The PLGA we use has a molecular weight between 50,000 and 75,000 g/mol with a lactic acid to glycolic acid ratio of 85:15 (Sigma-Aldrich catalog#:430471). This results in a slower degradation time. The half-life degradation time of PLGA can be increased to more than 3 months while the 50:50 ratio PLGA has the shortest half-life of less than 2 weeks. [33] The degradation of PLGA occurs in the presence of water due to hydrolysis of the ester linkage in PLGA.

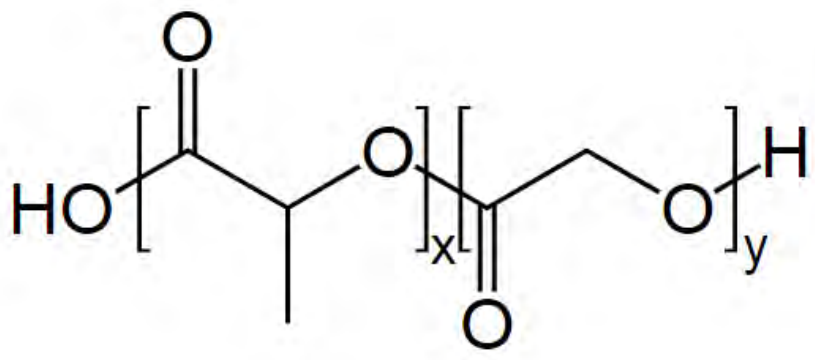

Figure 1.6 PLGA structure.

The degradation of the polymer will change the properties and morphology of the particles. Thus, avoiding particle degradation during the time scales of our experiments is very important. The PLGA nanoparticles dispersed in water should be centrifuged, frozen and lyophilized as early as possible to prevent premature degradation.

1.6 Aging Effect

The aging effect can change the configuration of the polymer chains and this will cause the glass transition temperature to change. Usually, the aging effect will cause a large peak in the DSC scan due to the enthalpy of relaxation at the same location as the glass transition. However, the enthalpic relaxation peak can be separated out from the glass transition by TMDSC. The aging effect can be slowed down when stored at low temperature. It was researched that when stored frozen, the aging effect can be extensively slowed down. After the sample is lyophilized and frozen at a temperature lower than 0 °C, it can take 12 months before the aging effects to start to be obvious on the polymer structure and glass transition temperature. [34] Thus, low temperature

storage is highly recommended to significantly slow down the polymer aging in the nanoparticles.

1.7 Centrifuge

A centrifuge (Eppendorf centrifuge 5430) was used to purify and wash the resulting particles made by all three methods. The surfactant used for both nanoprecipitation and nanoemulsion is poly(vinyl alcohol) (PVA) (Sigma-Aldrich cat.#363073). PVA can dissolve in water while the PLGA cannot. When the sample is centrifuged, the PLGA particles dispersed in water will be pushed towards the outside of the vessel, while the PVA dissolved in the water will remain in the solution and cannot be centrifuged out. The vessel of samples is positioned with a certain angle toward the center of the rotor and this will cause the bottom of the vessel to become the most outward part of the vessel, leading to the samples being concentrated on the bottom of vessel. The supernatant will be the water with surfactant and the lower suspension will be the PLGA particles. By removing the supernatant, adding ultra-pure water inside and continuing to centrifuge for several times, the surfactant can be removed almost completely. [37] Very small particles will also be lost each time the samples get washed. Long centrifugation times are used to limit this loss of sample. For the electrospray jetting samples, the particles will also be washed using a centrifuge. As the particles produced by electrospray jetting tend to have a wider size distribution, the centrifugation process is slightly different. The sample will be centrifuged for a short time period (around 5 min) at a moderately lower speed to centrifuge out the large particles which are of very poor morphology. Then, the remaining supernatant will be centrifuged at high speed

for longer times and this will be repeated three times. The purpose of the final washing steps is to wash out the CTAB which is used to increase the conductivity of the solution.

1.8 NTA and SEM

Nanoparticle tracking analysis (NTA) is a convenient method to measure the nanoparticle size and concentration with the sizes between 10 nm and 2000 nm dispersed in solution. This technique utilizes the properties of light scattering and Brownian motion to acquire data of particle size and size distribution as well as the concentration. The sample will be injected into an observing chamber. A laser beam is emitted towards the chamber. Once the laser reaches the particle suspension, the light will be scattered in an easily observed manner which can be visualized via a magnification microscope. A camera is mounted inside to record a video of the movement of the scattered light from the particles. Then, the captured video will be analyzed by a developed tracking technique software. The software will use the Stokes-Einstein equation to calculate the diameter of the particles and form a size distribution graph:

$$\mathrm{D} = \frac{k_b T}{6\pi\eta r}$$

where D is the diffusion constant calculated from the particle tracks, k_b is Boltzmann's constant, T is the absolute temperature, η is the dynamic viscosity and r is the radius of the spherical particle. The function was published in Einstein's (1905) classic paper on the theory of Brownian motion.[35]

The NTA we use is the Nanosight NS300. It is important to control the concentration of samples tested under NTA. If the sample exceeds the concentration detection limit or is too low the resulting size data will be inaccurate. The suitable concentration for measurement by NTA is between 108 and 5x108 particles per ml.

The NTA we use is the Nanosight NS300. It is important to control the concentration of samples tested under NTA. If the sample exceeds the concentration detection limit or is too low the resulting size data will be inaccurate. The suitable concentration for measurement by NTA is between $1x10^7$ and $1x10^9$ particles per ml.

SEM (Scanning Electron Microscope) can be used to observe the nanoparticles' morphology. In a typical SEM, an electron beam is emitted from an electron gun to focus on the sample. When the primary electron beam interacts with the sample, the electrons will lose energy because of the energy exchange between the sample and the electrons, resulting in reflection, scattering and electromagnetic radiation. All of them can be detected by different types of detector. While the SEM has a moderately lower resolution when compared with other microscopy like transmission electron microscopy, it usually works faster and is convenient for PLGA sample observation.

1.9 Glass Transition Temperature

The glass transition is the phenomenon in polymers where there is a dramatic change in properties with temperature change. Polymer's usually consist of two different portions. They are the crystalline portion and amorphous portion. These two different portions give the polymer unique properties. The glass transition is one phenomena caused by the existence of the amorphous part.

The crystalline part in the polymer is where the molecules packs together with a certain repeated structure or certain order, for instance into chain folded lamellae. On the contrary, the molecules in the amorphous part are in a disordered state. The crystallinity is expressed as the total weight fraction or volume fraction of crystalline material.

The crystalline part gives rise to a melting temperature which is the temperature where the ordered structure comes apart and the polymer becomes a liquid. The amorphous part gives rise to the glass transition temperature which is the temperature where the disordered polymer chains begin to slide past one another allowing the polymer to begin to soften and flow. The glass transition temperature is usually a span of temperatures where the transition starts and finish, and the midpoint of that span is usually used as the glass transition temperature. Before the glass transition, the chains of the amorphous polymer remain tangled with each other and frozen in place. The molecules or chains move with extremely slow speed. During the glass transition, the chains start to move faster and begin to escape the entanglements with each other. After the glass transition, the chains move freely and thus no longer stick together allowing the chains to fully relax. Differential scanning calorimetry (DSC) is used to measure the glass transition temperature. The glass transition appears as a step change due to the change in heat capacity between the glass and rubbery polymer. The glass transition is usually accompanied by some enthalpic relaxation which can be observed as a peak in the DSC curve superimposed upon on the glass transition.

1.10 DSC

Differential scanning calorimetry (DSC) is a technique used for thermal analysis. The working mechanism is illustrated below. The sample will be sealed within a metal pan using a press. An empty pan which is also sealed will be used as the reference pan. Both the sample pan and the reference pan will be placed in an isolated chamber within the DSC. Both pans will be heated at the same heating rate which is set by the user. An inert purge gas, typically nitrogen, will be injected into the chamber at a constant rate which is set by the software. [36]

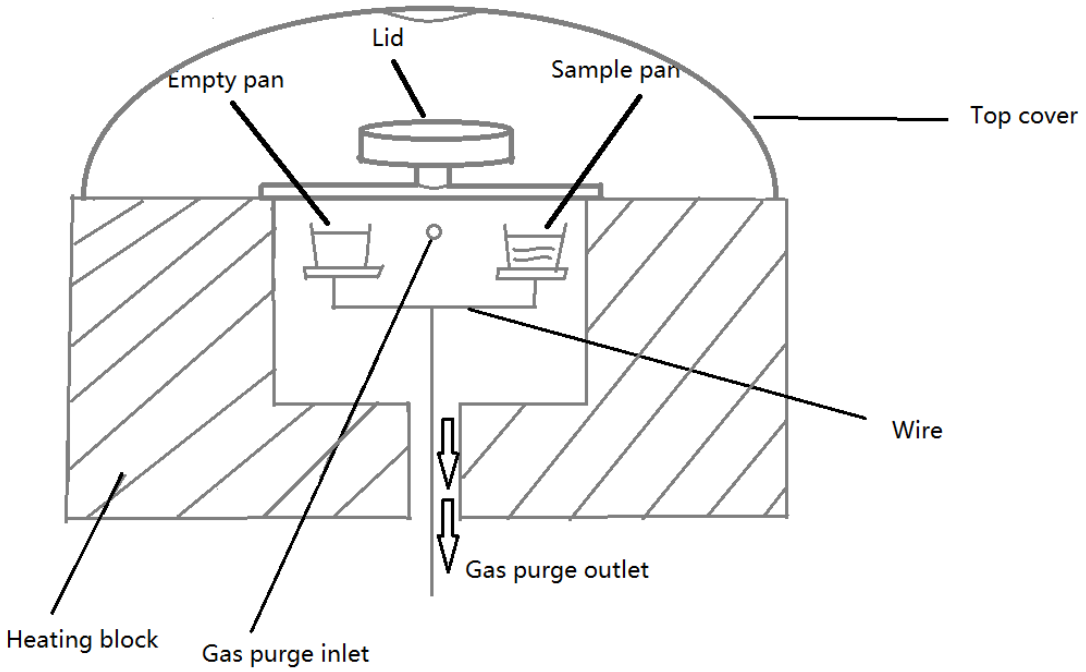

Figure 1.7 Example of how DSC works.

The heat provided to both reference and sample pans will be recorded separately by the DSC and the DSC is designed to provide a stable heat and make sure the temperature of both pans can increase stably according to the set heating rate. Different

DSC companies have different designs for this mechanism. [29] A well-designed DSC can provide a stable heat flow. Due to the existence of sample inside the sample pan, the heat absorbed by the sample pan will be higher than the reference pan. By using this difference, the heat absorbed by the sample can be calculated directly. As the sample is being heated and the temperature increases at a constant rate, thermal transitions happen at the same time. Due to the existence of thermal transitions, the heat absorbed by the sample will vary at different temperatures and transition processes. This change in the heat absorbed allows for the formation of a traditional DSC curve. The x-axis is usually the temperature and the y-axis is the heat flow which is recorded by the DSC. If a transition happened during a temperature range, there will be a difference on the recorded heat flow. This DSC technique makes the study of thermal transitions possible. However, there are several disadvantages of DSC. For example, when the sample used is a sample that has aged, the DSC results will have a very big enthalpic relaxation peak overlapping with the glass transition. To overcome this problem, researchers usually ignore the first heating results. Instead, they take data from the cooling run or second heating run, because thermal history, such as the aging effect, can be erased by making the sample fully relaxed. However, this practice of throwing out the first heating run means researchers can hardly research the thermal history. Even if they try to get data from the first heating run from DSC, they can't get accurate results. When several transitions happen over a short temperature span, the results will simply be the overlapping of these transitions and conventional DSC cannot separate them. The following is an example of conventional DSC results.

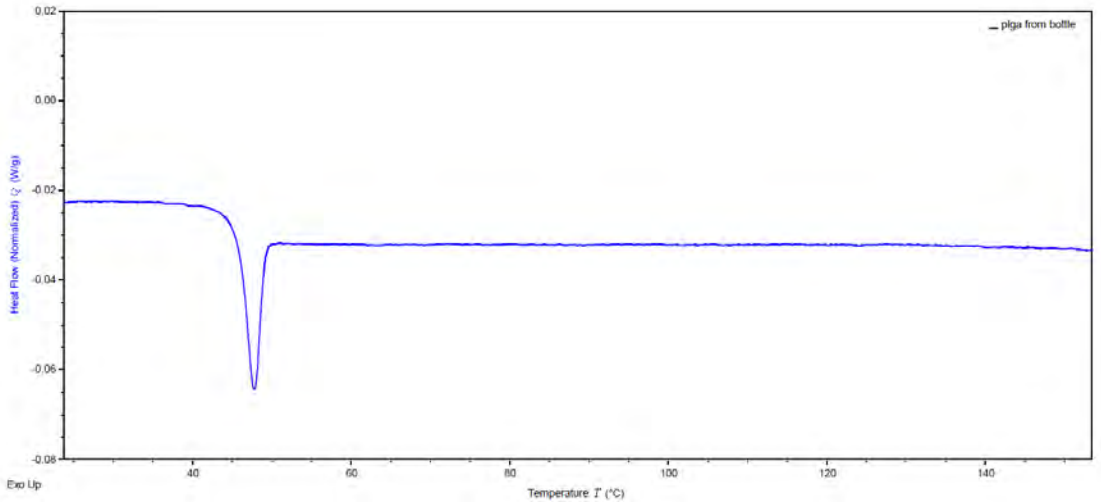

Figure 1.8 Example of conventional DSC results with PLGA sample.

This is an example of a first heating cycle with a glass transition temperature. Only the total heat flow curve can be observed for each heating/cooling process so the enthalpic relaxation peak due to polymer aging is superimposed upon the step change of the glass transition, making it impossible to accurately measure.

1.11 TMDSC

Temperature modulated differential scanning calorimetry (TMDSC) is designed to overcome the problems of conventional DSC. Since the conventional DSC can't separate important overlapping transitions, several new mechanisms are developed to overcome this weakness. For example, the TMDSC developed by TA Instruments and Step Scan technique TMDSC developed by PerkinElmer are two different kinds of TMDSC. For the TA Instruments DSC, the total heat flow is separated into two different flows, the reversing flow and the non-reversing flow. The conventional DSC can only calculate the Cp dT/dt part. But it can't calculate the later f (T, t) part. The function used for DSC is below:

$$\frac{dH}{dt} = Cp\frac{dT}{dt} + f(T,t)$$

Where dH/dT is total heat flow rate (mW, which is mJ/s), Cp is sample heat capacity which is specific Cp multiplied by sample mass (J/°C), dT/dt is the heating rate (°C/min) and f(T,t) is heat flow that is a function of temperature and time.

The whole function is considered to be the total heat flow. It is divided into two different parts. The Cp part is the reversing flow. The other part which is a function of temperature and time is the non-reversing flow.

Conventional DSC cannot separate the kinetic part which is the function of Cp and dT/dt and non-kinetic part which is the function of temperature and time. However, TMDSC can separate them. The difference is TMDSC usually uses a fluctuated heating rate instead of the constant heating rate. The heating rate has a certain amplitude, period and average heating/cooling rate. Also, different TMDSC from different companies use different methods of modulating the temperature. Some of them use a sine function, while others use cosine and other fluctuating functions. There are also different temperature modulated DSC using different techniques like Step Scan. Step Scan is a technique using different modulated functions than a sinusoidal function, but due to lack of software support, Step Scan based DSC cannot fully separate out the enthalpic relaxation and glass transition. Thus, it is still the same as conventional DSC on this point.

In conventional DSC, heat capacity (Cp) is determined by dividing the heat flow by the heating rate as displayed below:

$$\mathrm{Cp} = K_{Cp} \times \frac{Heat\ Flow(Sample) - Heat\ Flow(Blank)}{Heating\ Rate}$$

where K_{Cp} is the calibration constant. Cp can also be calculated by comparing the difference in heat flow between two runs with the same sample at two different heating rates. [36] But this method is usually not practical.

$$\mathrm{Cp} = K_{Cp} \times \frac{Heat\ Flow\ at\ Heat\ Rate\ 2 - Heat\ Flow\ at\ Heat\ Rate\ 1}{Heating\ Rate\ 2 - Heating\ Rate\ 1}$$

However, in modulated DSC, the heat flow is not constant. By using a sine function fluctuated heating/cooling rate, it collects both the constant heating/ cooling rate information and the fluctuated information. By collecting both types of information, the above calculation becomes practical because it can easily get information from many different heating rates within the same run.

$$\mathrm{Cp} = K_{Cp}(Q_{amp}/T_{amp})(Modulation\ Period/2\pi)$$

where Cp is heat capacity, K_{Cp} is heat capacity calibration constant, Q_{amp} is heat flow amplitude and T_{amp} is temperature amplitude. [36] By using the discreet Fourier transformation technique, the above equation can be calculated and used for TMDSC to calculate a sample's Cp.

By calculating the Cp, the reversing flow (Cp dT/dt part) can also be calculated. While the fluctuated temperature change rate has an average rate, it can also be used to get the dH/dt which is the total heat flow. By using the total heat flow minus the reversing flow, the non-reversing flow (f (T, t) part) can also be calculated. Three

different curves can now be observed in the DSC plot: the total heat flow, the reversing heat flow and the non-reversing heat flow. After the sinusoidal modulated curve is simplified, TMDSC data appears like the below image.

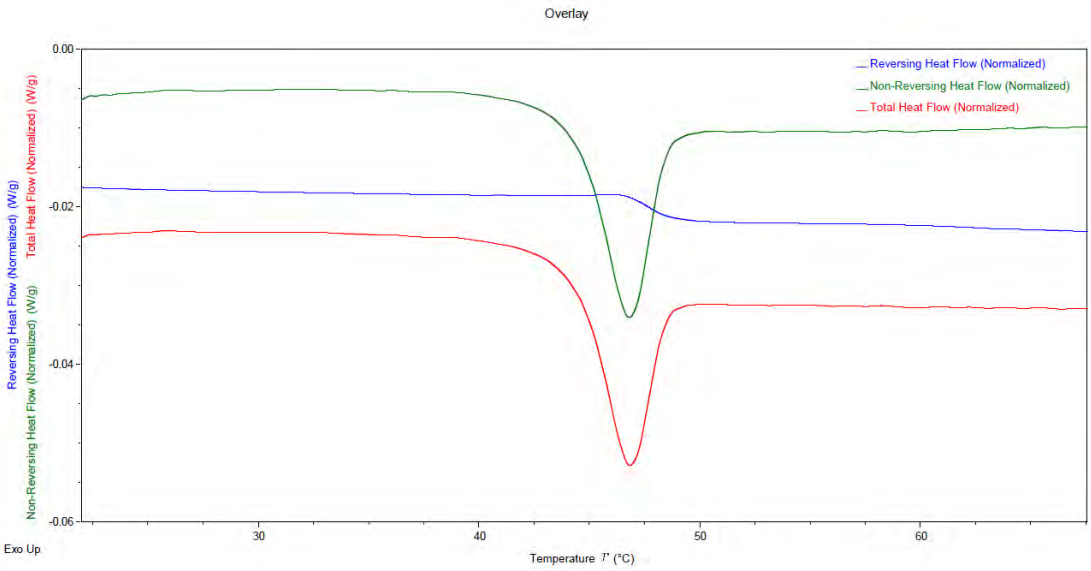

Figure 1.9 Example of TMDSC results with PLGA sample.

For each heating and cooling run, three different curves can be observed. The green one in the image is the total heat flow, the blue one is the reversing flow, while the red one is the non-reversing flow. It is obvious that it separates out processes like enthalpic relaxation from the glass transition, as well as other transformations such as crystal perfection and melting.

The reversing flow usually contains information about glass transition temperature. Non-reversing flow usually contains information about kinetic properties like melting crystallization and enthalpic relaxation.

1.12 Effect of Thermal History on Glass Transition Temperature (Tg)

Once the size optimization is done, nanoparticles of same size but with different thermal history which are made from three different methods or with the same type method which uses different recipes. The comparison of Tg on the first heating/cooling process between these sample will provide evidence of thermal history's effects.

CHAPTER 2

PROCEDURE, OPTIMIZATION AND RESULTS

2.1 Procedure of Nanoprecipitation

For the nanoprecipitation method, there are many factors which can be used to control the size of the particles. The surfactant concentration and the organic phase concentration were chosen as variables. It is observed that increased surfactant concentration can lead to the size decreasing initially, but the size will start to increase once the concentration reaches a certain value. This means it is possible to have two different concentration of surfactant resulting in the same particle size.

To create nanoparticles by nanoprecipitation, around 20 to 25 mg of PLGA (MW:50000-75000) was weighed and dissolved inside 2 ml of acetone solution to create the organic phase. Varying amounts of PVA (200 mg – 2500 mg) were dissolved inside 100 ml of ultra-pure water to create the aqueous phase. The organic phase was then injected into the aqueous phase under stirring. The sample was stirred overnight to evaporate all the organic solvent. Then, the samples were collected with a filter with pore size of 40 um to remove the large debris. The samples were centrifuged using the maximum speed of the centrifuge 7,745 × g (7,830 rpm). The supernatants containing PVA were removed and the pellet samples were resuspended in pure water and recentrifuged. This was repeated four times to wash away the PVA. The samples were replenished to 40 ml to keep volume constant. 2 ml of sample after the final centrifuge was removed for analysis by NTA and SEM. Then, the samples were frozen at -70°C and lyophilized. Finally, the samples were tested using TMDSC.

2.2 Procedure of Nanoemulsion

To create nanoparticles by nanoemulsion, around 20 to 25 mg of PLGA (MW:50000-75000 g/mol) was weighed and dissolved inside 1 ml of chloroform to create the organic phase. Varying amounts of PVA (40 mg – 200 mg) were dissolved inside 8 ml of ultra-pure water to create the aqueous phase. The organic phase was injected into the aqueous solution. Then, the mixtures were sonicated using an amplitude of 100 (around 17 J energy), in pulses that were 1 second long with 4 seconds in between pulses. The sonication procedure lasted for 30 mins of pulse time, which in sum is 150 mins total process time. After sonication, the sample were stirred overnight to evaporate the chloroform. They were washed four times via centrifugation to remove the PVA, following the same washing procedure used for nanoprecipitation. 2 ml of the sample was removed for analysis by NTA and SEM. The remaining sample was frozen and lyophilized for TMDSC tests.

2.3 Procedure of SEM

In order to make sure the morphology of the nanoparticles is good, samples made from nanoprecipitation, nanoemulsion and electrospray jetting were imaged by SEM. This is especially useful for the electrospray jetting samples because the jetting process is often unstable, requiring careful control of the voltage. Otherwise, the jetting process will produce many fibers or poor morphology particles instead of nanoparticles. Thus, the way to check if the jetting process worked well is to image the resulting samples with SEM. Small pieces of aluminum foil previously left on the collecting plate were collected after jetting and stuck onto the surface of an SEM sample holder using adhesive tape. For nanoemulsion and nanoprecipitation samples, a droplet of particle

solution was placed on a small piece of aluminum foil and allowed to dry overnight. Then, the sample was coated using carbon cord to create a conductive surface on the sample. After the coating process, the sample holders were placed inside the SEM observation chamber and imaged.

2.4 Procedure of Electrospray Jetting Optimization

One of the major issues with jetting is that it's very unstable and very sensitive to the surrounding environment. Thus, an optimization step to create a stable jetting method is required. Three different recipes were prepared to test the stability of jetting. The first recipe uses 10% of PLGA (MW:50000-75000) and 5% of CTAB (Sigma-Aldrich cat.# H9151) dissolved in an organic solution which consists of a 6 to 4 ratio of chloroform to DMF. The second recipe uses 1% of PLGA and 0.5% of CTAB, keeping the ratio of PLGA to CTAB the same, dissolved in an organic solution which consists of a 1 to 1 ratio of chloroform to DMF. The third recipe uses 1% of PLGA and 0.5% of CTAB, again keeping the ratio of PLGA to CTAB the same, dissolved in an organic solution which consists of a 6 to 4 ratio of chloroform to DMF. The syringe pump speed is 0.2 ml/hr.

2.4.1 Jetting Results

For the first recipe, despite adjusting the voltage, the Taylor cone cannot be properly formed and jetting did not result in any nanoparticles. Instead the first recipe produced fibers. The second recipe is far better than the first one, however, fiber production is still a large portion of the sample. Though the increase percentage of DMF can lead to better uniformity, the stability was also decreased. The Taylor cone during the process

is not stable with the higher percentage of DMF. The third recipe is better for nanoparticle production than the second one. The jetting is more stable than the second recipe and the produced samples consists of less fibers. Once the Taylor cone formed, it required almost no adjustment of voltage to keep it stable. Thus, the third recipe was chosen as the optimal recipe.

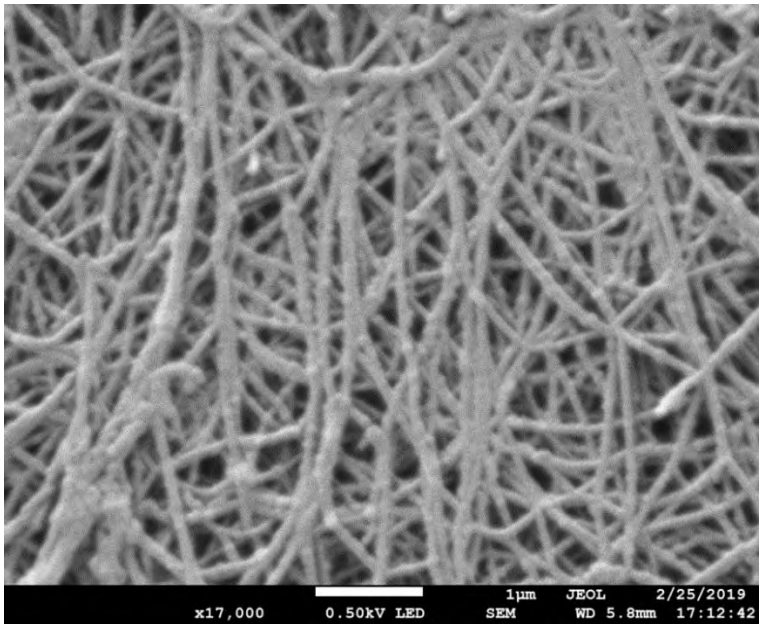

Figure 2.1 First recipe jetting image of SEM with PLGA.

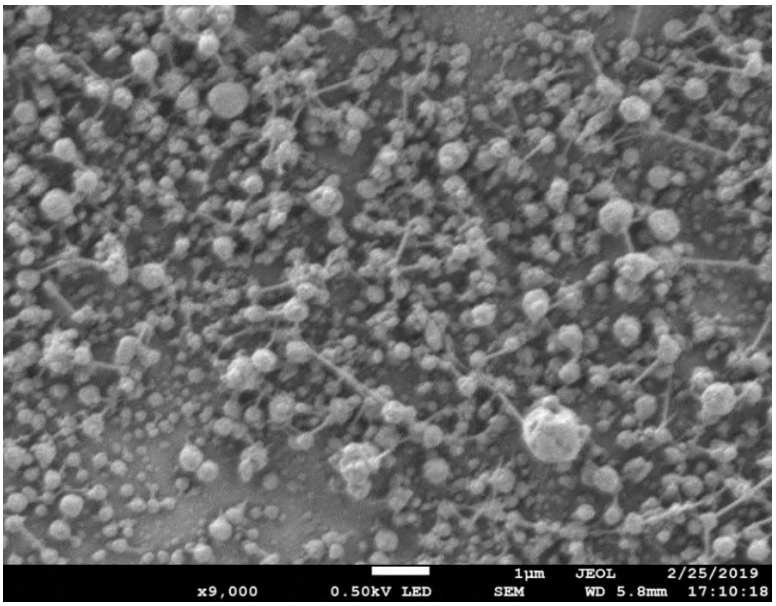

Figure 2.2 Second recipe jetting image of SEM with PLGA.

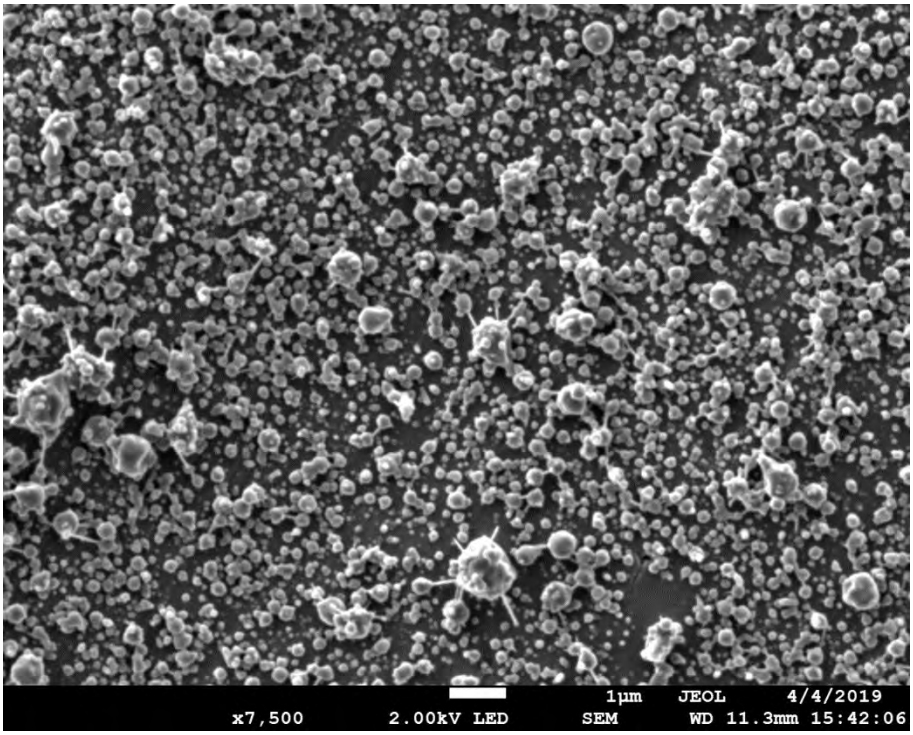

Figure 2.3 Third recipe jetting image of SEM with PLGA.

2.4.2 Further Optimization of Electrospray Jetting

From the SEM images, it is obvious that the samples made by jetting can be further optimized. The morphology of the samples is relatively poor with fibers and large debris that needs to be removed or at least reduced. The jetting sample is also of low production efficiency. Further optimization to the jetting process was made.

Several different recipes were selected. The first recipe uses the third recipe from the previous section, but with the injection speed reduced to 0.1 ml/hr. The second recipes use a different ratio of organic phase with a 7:3 ratio of chloroform to DMF with 0.1 ml/hr injection speed. The third recipe use a 4:1 ratio of chloroform to DMF with the same injection speed. The fourth recipe use a 9:1 ratio of chloroform to DMF with same injection speed.

2.4.3 Jetting Results of Further Optimization

The first recipe with the injection speed reduced by half (6:4 of chloroform to DMF) leads to better results. The fibers which can be noticed easily in the previous samples are not present in these samples. The portion of nanoparticles with diameters around 100 nm is significantly increased. The amount of large debris is significantly reduced as well. The second recipe doesn't have significant improvement, but it is obvious from observation that the portion of nanoparticles with 100 and 200 nm size increases gradually and fibers can hardly be observed. The forth samples have significant improvements. The size uniformity increased a lot. The majority of particles have become nanoparticles with a size of 100 nm and 200 nm which is consistent with the size distribution of later discussed nanoemulsion and nanoprecipitation samples. Thus, the forth recipe with a ratio of chloroform to DMF being 9 to 1, was chosen as the final optimal recipe for DSC testing. Due to lack of enough mass of jetted particles and limited access to a DSC, the jetting samples were not tested by DSC or NTA, but they will be included in the future.

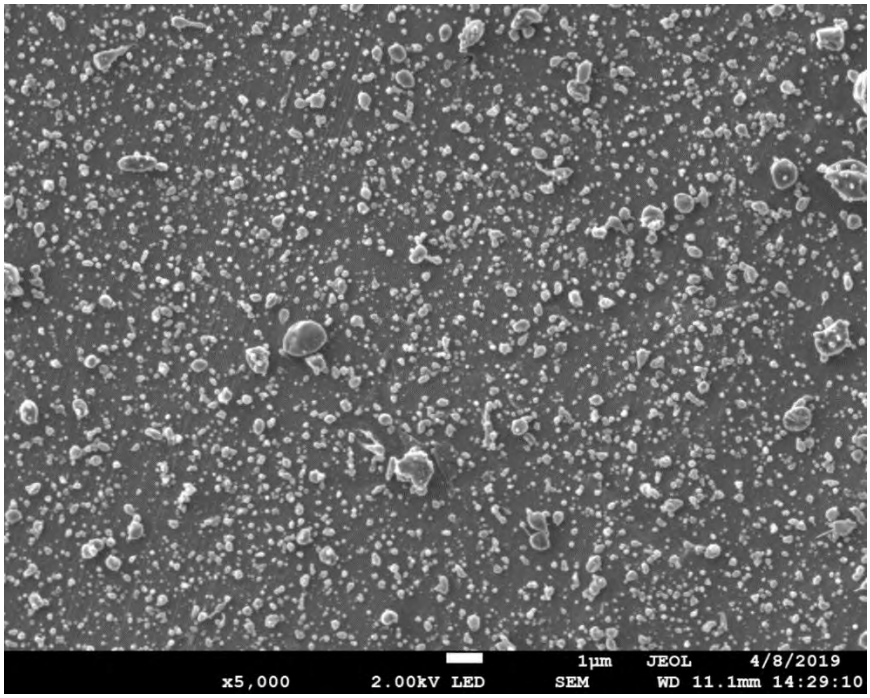

Figure 2.4 First recipe jetting image of SEM with PLGA with half jetting speed.

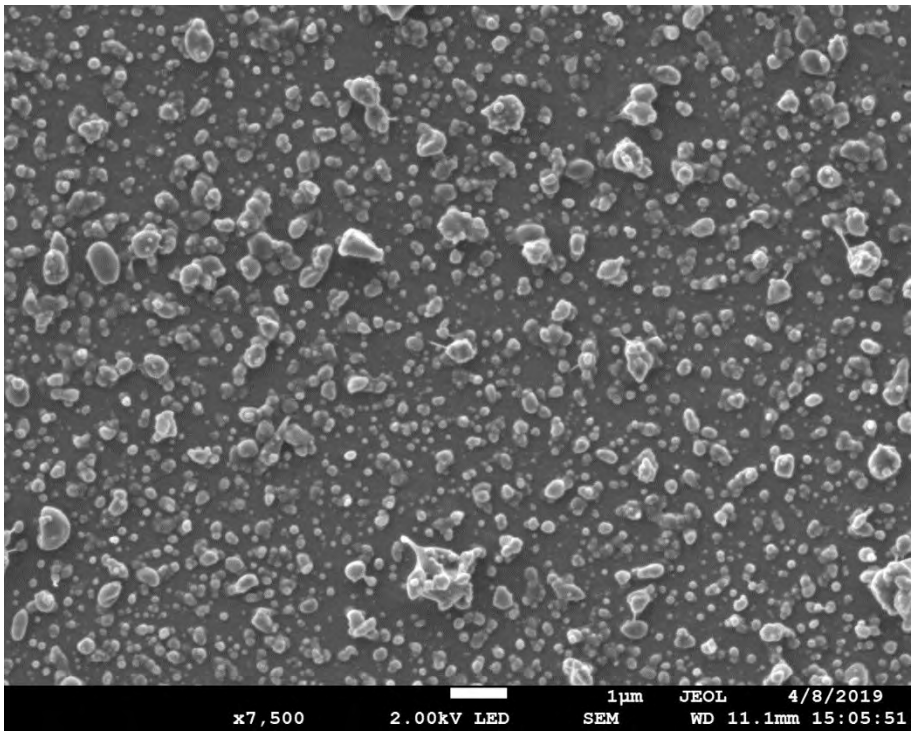

Figure 2.5 First recipe jetting image of SEM with PLGA with half jetting speed.

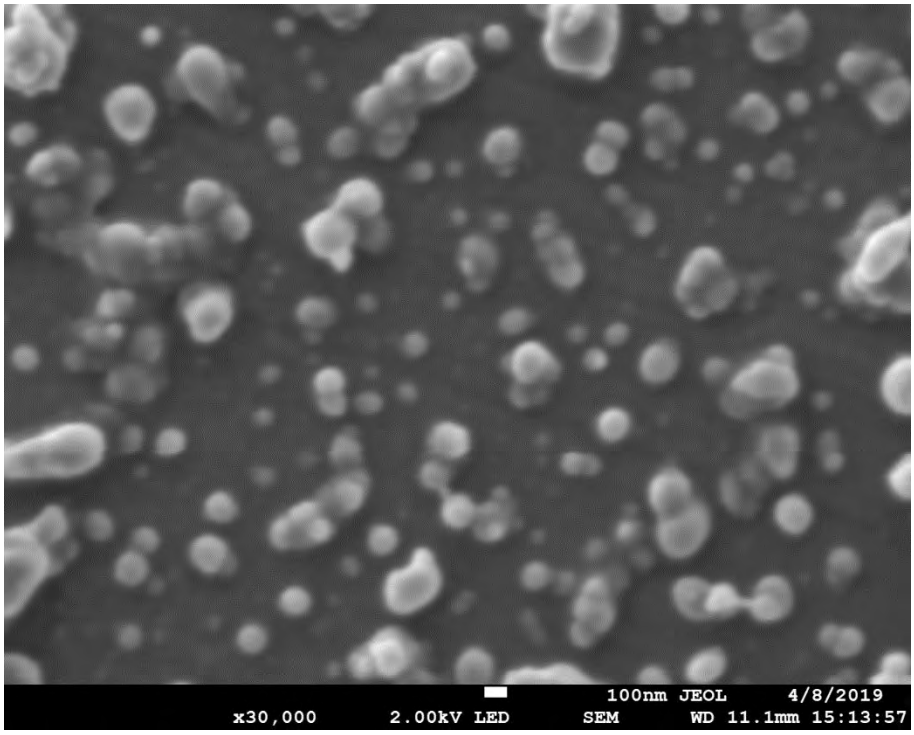

Figure 2.6 First recipe jetting image of SEM with PLGA with half jetting speed.

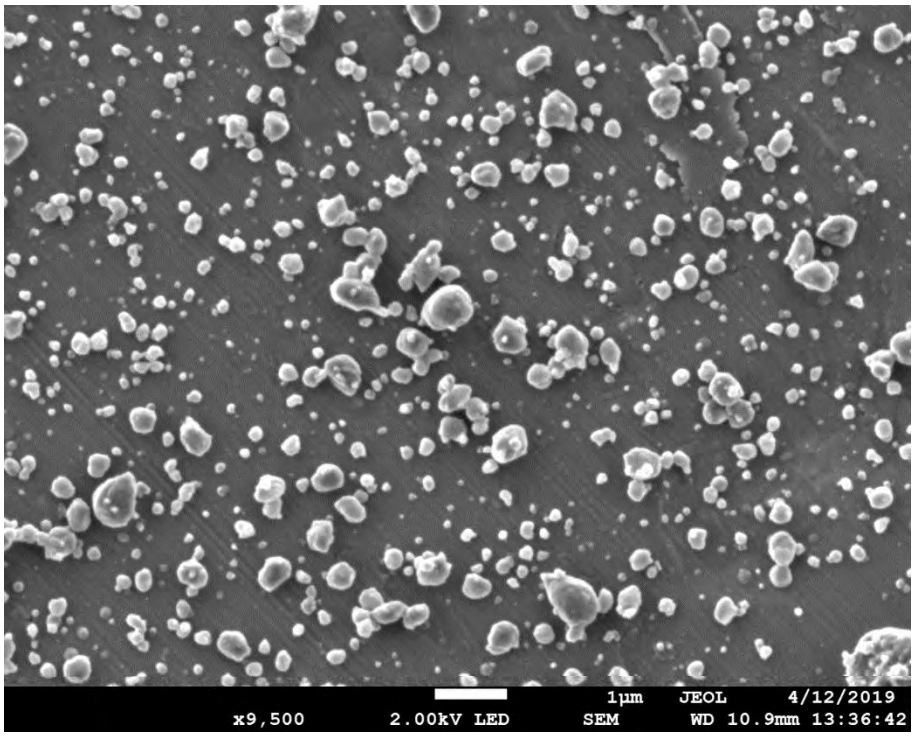

Figure 2.7 Second recipe jetting image of SEM with PLGA with half jetting speed.

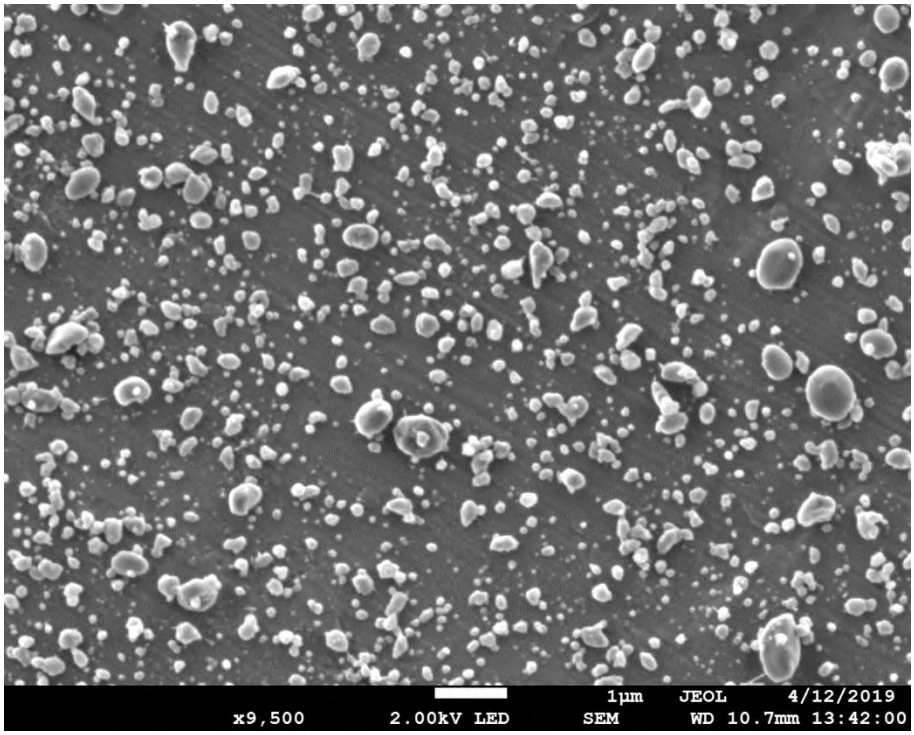

Figure 2.8 Third recipe jetting image of SEM with PLGA with half jetting speed.

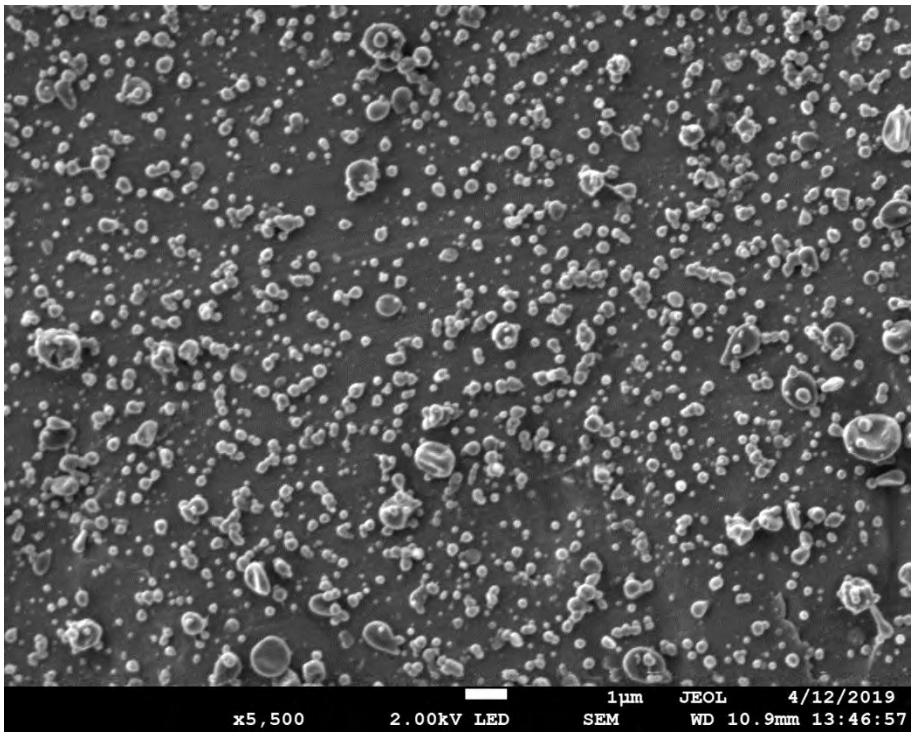

Figure 2.9 Fourth recipe jetting image of SEM with PLGA with half jetting speed.

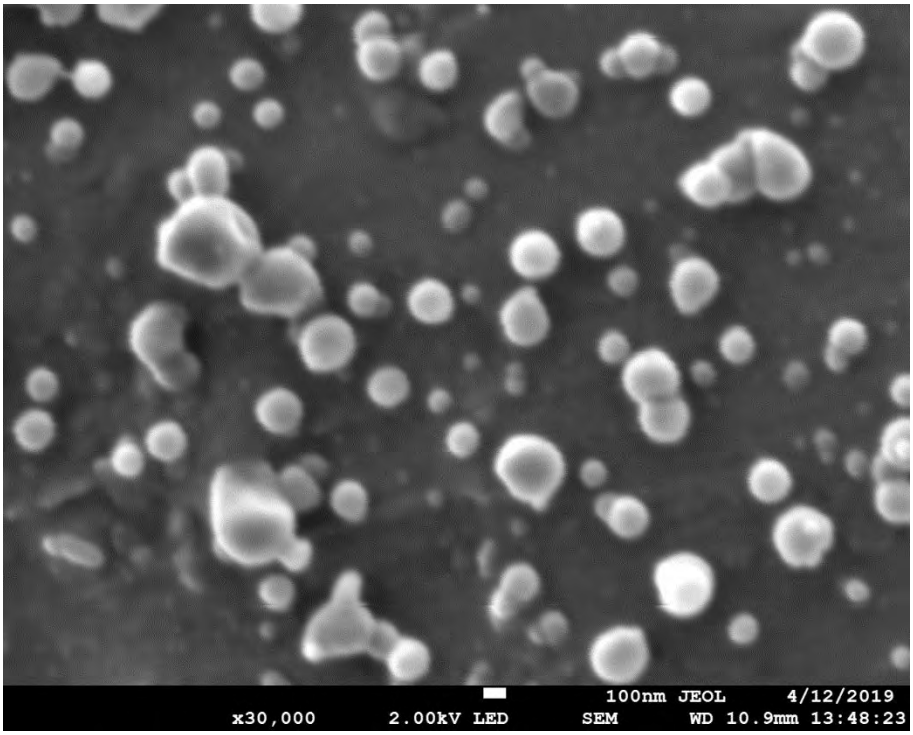

Figure 2.10 Fourth recipe jetting image of SEM with PLGA with half jetting speed.

2.5 SEM Results of Nanoemulsion and Nanoprecipitation Samples

Nanoprecipitation samples have good spherical morphology under SEM. Due to charging problems with the SEM, images at high magnification are blurry and the15 nm carbon coating is not sufficient. Other coatings like gold coating are recommended and probably available in future experiments. Some big aggregates are observed but the majority of particles remain around 100 nm and this size is consistent with NTA results.

Nanoemulsion samples have the same charging problems in the SEM as the nanoprecipitation samples, but they are of good spherical morphology. The size results are also consistent with NTA results. A notable difference for the nanoemulsion process is the production of a few larger particles while the “larger particles” from nanoprecipitation are more likely to be aggregates of smaller particles.

Jetting samples have a very small portion of fiber-like material and large debris and have relatively poor morphology. One possibility for this is because the PLGA used is of high molecular weight. Despite this, majority of the nanoparticles with a diameter around 100 nm are still of good morphology. However, electrospray jetting has a low production efficiency decreasing the total amount of nanoparticles produced.

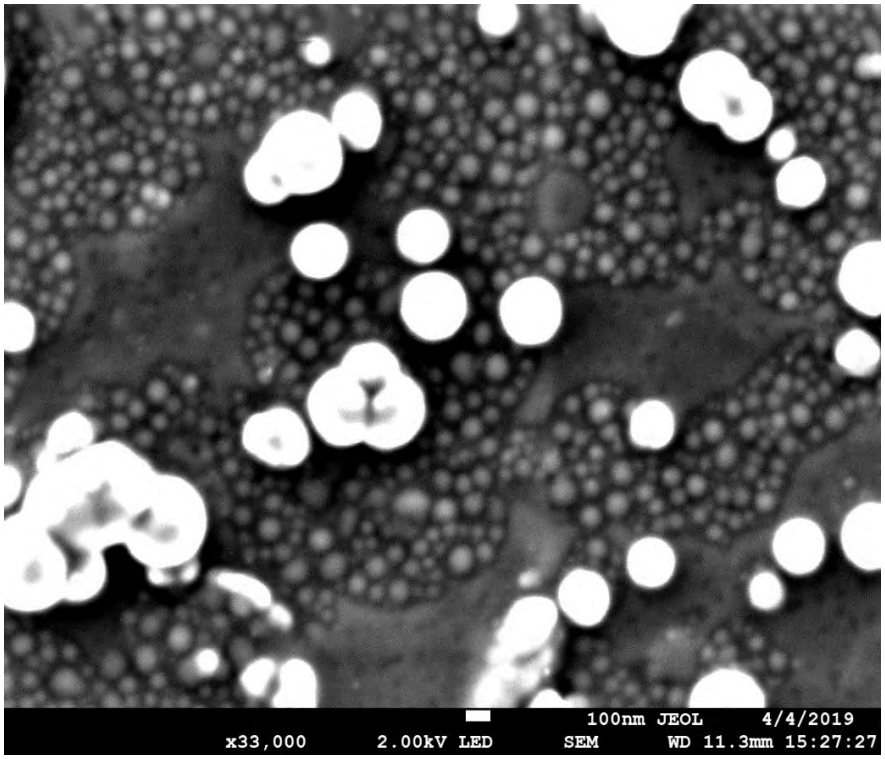

Figure 2.11 Nanoprecipitation sample SEM image.

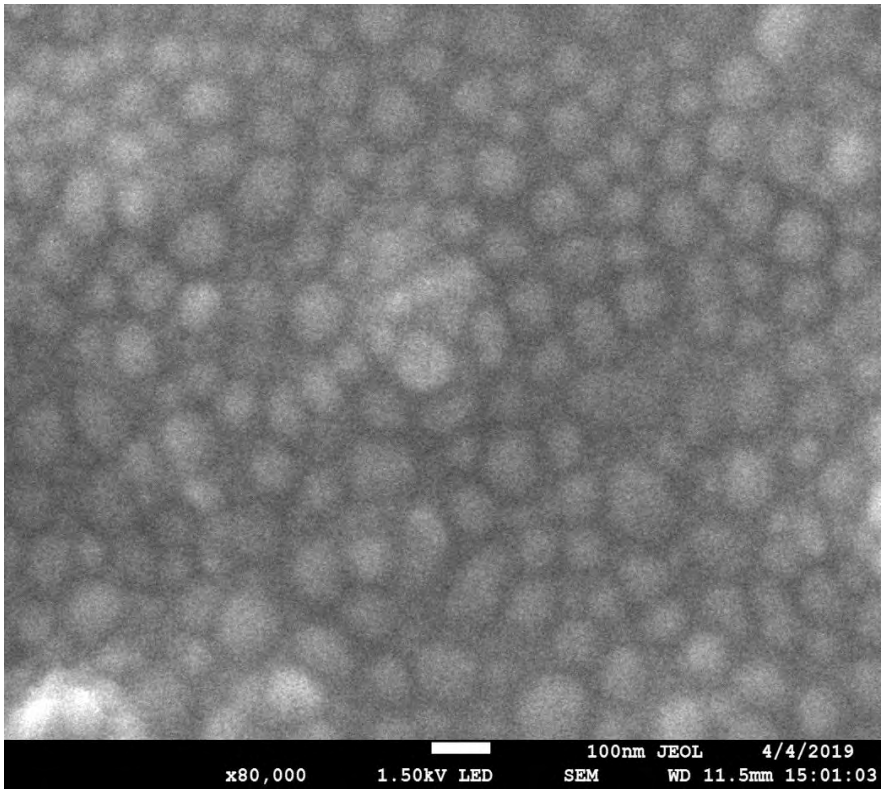

Figure 2.12 Nanoprecipitation sample SEM image.

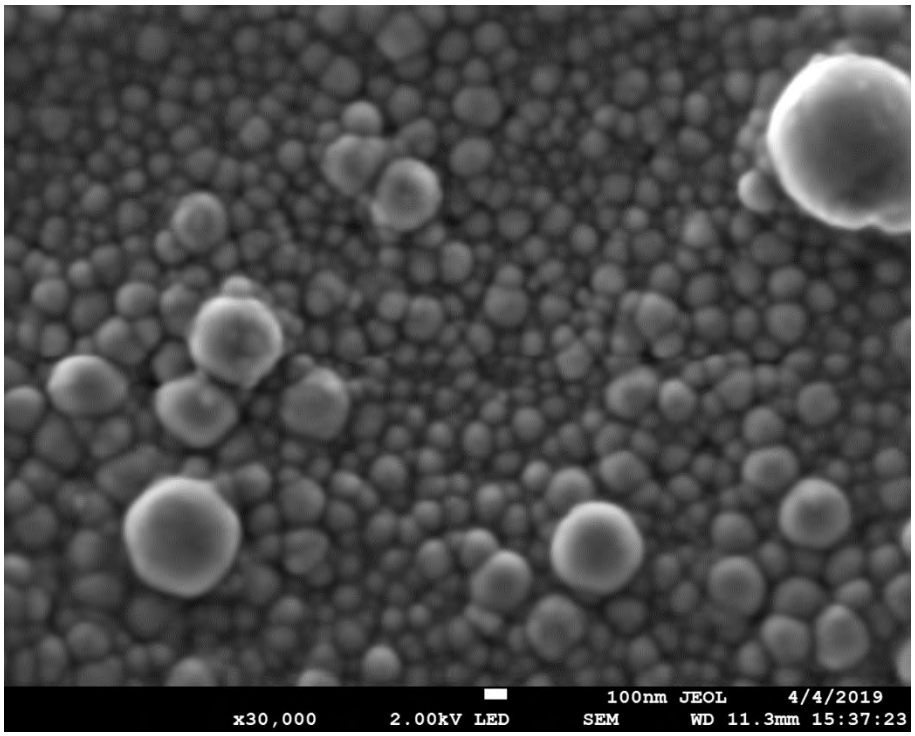

Figure 2.13 Nanoemulsion sample SEM image.

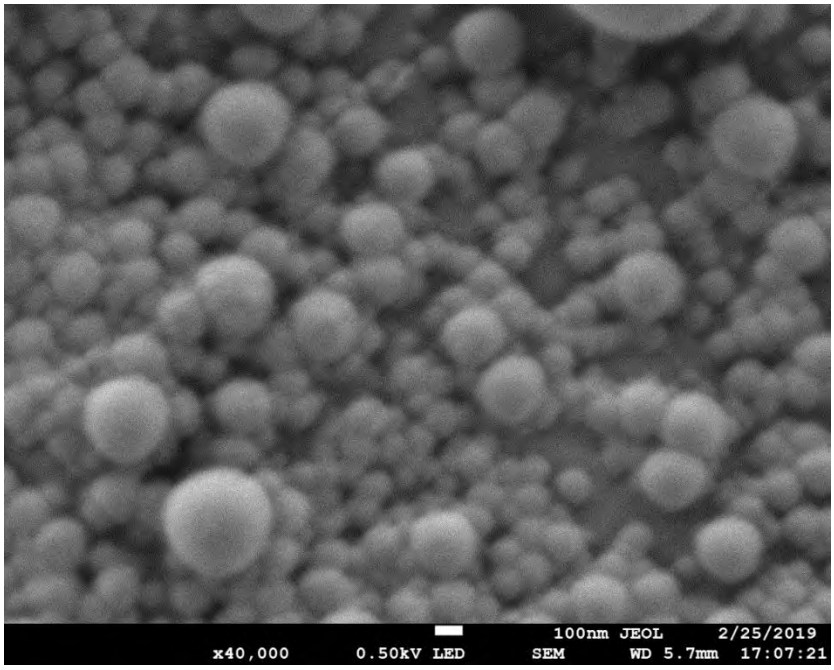

Figure 2.14 Nanoemulsion sample SEM image.

2.6 Procedure of NTA

2 ml of the particle suspension was removed after the washing steps. The sample was diluted between 100 to 1000 times to make the concentration of PLGA nanoparticles suitable for NTA testing. Samples were then tested for their size distribution using NTA. The syringe pump was initially started with 1000 au injection rate until particles started to move on the screen. Then the injection speed was decreased to 100 au to provide a stable flow. Five videos were captured that were each 1 min long for each sample. Then the videos were analyzed using the NTA software.

2.7 Procedure of NTA Data Analysis

All the individual videos marked by the NTA software as containing high vibration are not considered reliable data and were not used. For each data set consisting of any high

vibration video, the data of average values and standard errors were recalculated after excluding the high vibration data. Moderate and minor vibration are within the NTA's acceptable range and were used for data analysis. Most of the data collected, however, do not contain any vibration in the videos. The concentration of the particles was plotted against the particle diameter to observe the size distribution of the particle samples.

2.8 Effect of Sonication Time at 0.5% PVA Concentration

The optimization of size started with the sonication time. Several samples consisting of 20 to 25 mg of PLGA (MW:50000-75000 g/mol) dissolved in 2 ml organic phase were prepared, injected into aqueous phase with 0.5% PVA concentration and sonicated for 1 min, 15 mins, 20 mins and 30 mins. Results are below:

Table 1.1 Nanoemulsion Sonication Time Effect on Mode and Mean Size under 0.5% PVA

Sonication time	**Mode Size(nm)**	**Mean Size(nm)**
1 min	226.9 +/- 25.5	266.6 +/- 4.2
15 mins	166.2 +/- 24.2	180.0 +/- 2.9
20 mins	142.1 +/- 2.5	163.7 +/- 0.4
20 mins repeat	137.2 +/- 4.2	156.5 +/- 2.1
20 mins average	139.6 +/- 3.3	155.1 +/- 1.2
30 mins	111.0 +/- 5.1	122.9 +/- 1.7
30 mins repeat	107.9 +/- 5.1	126.0 +/- 3.9
30 mins average	109.4 +/- 5.1	124.4 +/- 2.8

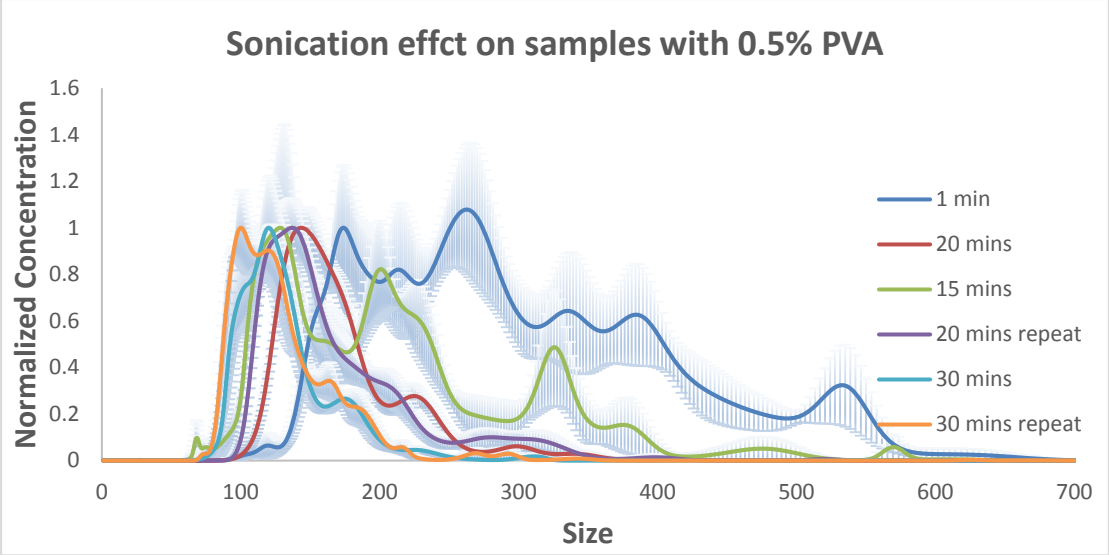

Figure 2.15 Emulsion sample with 1 min, 15 mins, 20 mins, 30 mins sonication and repeats under 0.5% PVA concentration.

It is obvious that under 0.5% PVA concentration, the sonication time significantly increased the uniformity of the size distribution and decreased the mean size. 1 min sonication leads to several huge peaks within the range of 100 nm to 600 nm and large particles around 550 nm were detected. 15 mins sonication leads to several peaks as well, though the peak range was reduced to the range 100 nm to 400 nm. Still, the size distribution is very polydisperse. However, after the sonication time was increased to 20 mins, the size uniformity was significantly improved with a large peak around 150 nm and a small peak on 220 nm and the size range was limited to 100nm to 300nm. The sonication time was further increased to 30 min and the continued improvement on size uniformity and decrease on mean size was observed. A small percent of nanoparticles even reached below 100 nm and the size range was limited to almost below 200 nm. Thus, 30 mins was selected as the suitable sonication time. It is an effective sonication time for the size optimization even for the samples with low surfactant concentration.

2.9 Effect of Sonication Time at 1% PVA Concentration

After the previous section, we want to further investigate the effect of sonication time on different surfactant concentration. Thus, several samples were prepared with PVA concentration increased from 0.5% to 1%. Other variables remained the same. The samples were sonicated with 1 min, 5 mins and 10 mins. The results are listed below:

Table 1.2 Nanoemulsion Sonication Time Effect on Mode and Mean Size under 1% PVA

Sonication time	**Mode Size(nm)**	**Mean Size(nm)**
1 min	177.6 +/- 11.6	198.9 +/- 1.4
5 mins	152.4 +/- 2.3	165.5 +/- 0.9
10 mins	145.8 +/- 2.3	151.0 +/- 1.3

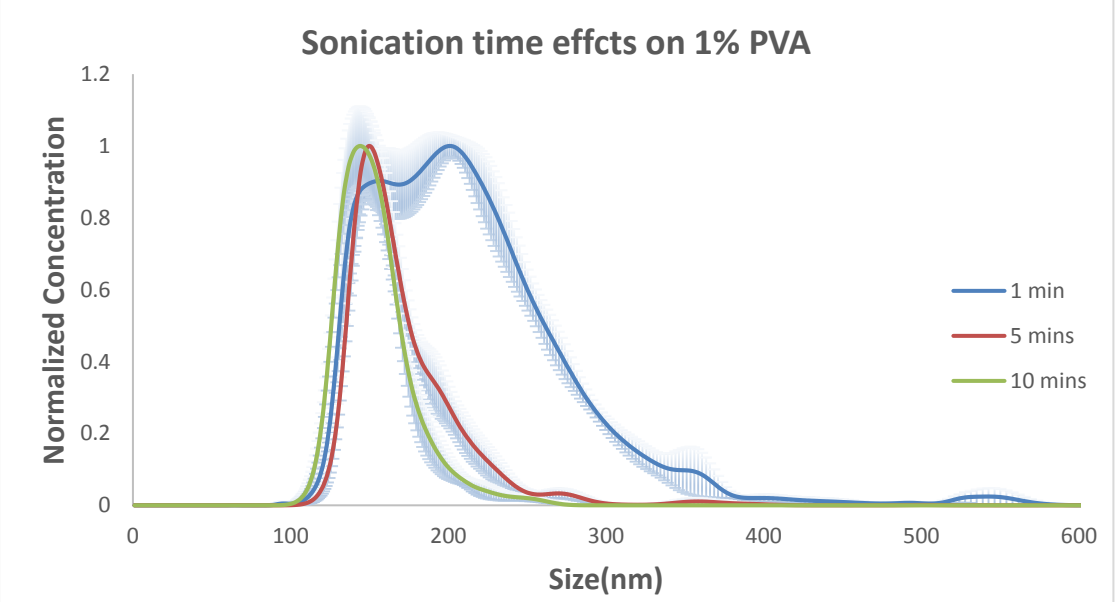

Figure 2.16 Emulsion sample with 1 min, 5mins and 10 mins sonication and 1% PVA concentration.

It can be observed that once the PVA concentration was increased to 1%, the size distribution of nanoparticles becomes more monodisperse than samples with 0.5% PVA concentration. Still, when the sonication time increases, the size uniformity also improves. The 1 min sonication sample resulted in a size range of 100 nm to 400 nm. 5 min sonication results in particle sizes ranging from 100 nm to 300 nm. 10 min sonication decreases the size further, limiting the size range to between 100 and 250 nm in a single peak. Thus, if the PVA concentration is 1%, 10 min sonication should be enough to produce nanoparticles with small size and good size distribution. For latter samples with 1% or higher PVA concentration, 30 mins sonication is used in order to remain consistent.

2.10 Effect of PVA Concentration on Nanoemulsion Samples

Different PVA concentration was tested and replotted below and all those samples will be tested under TMDSC in the future. The PVA concentration ranges from 0.5% to 2.5%. Other variables remained the same.

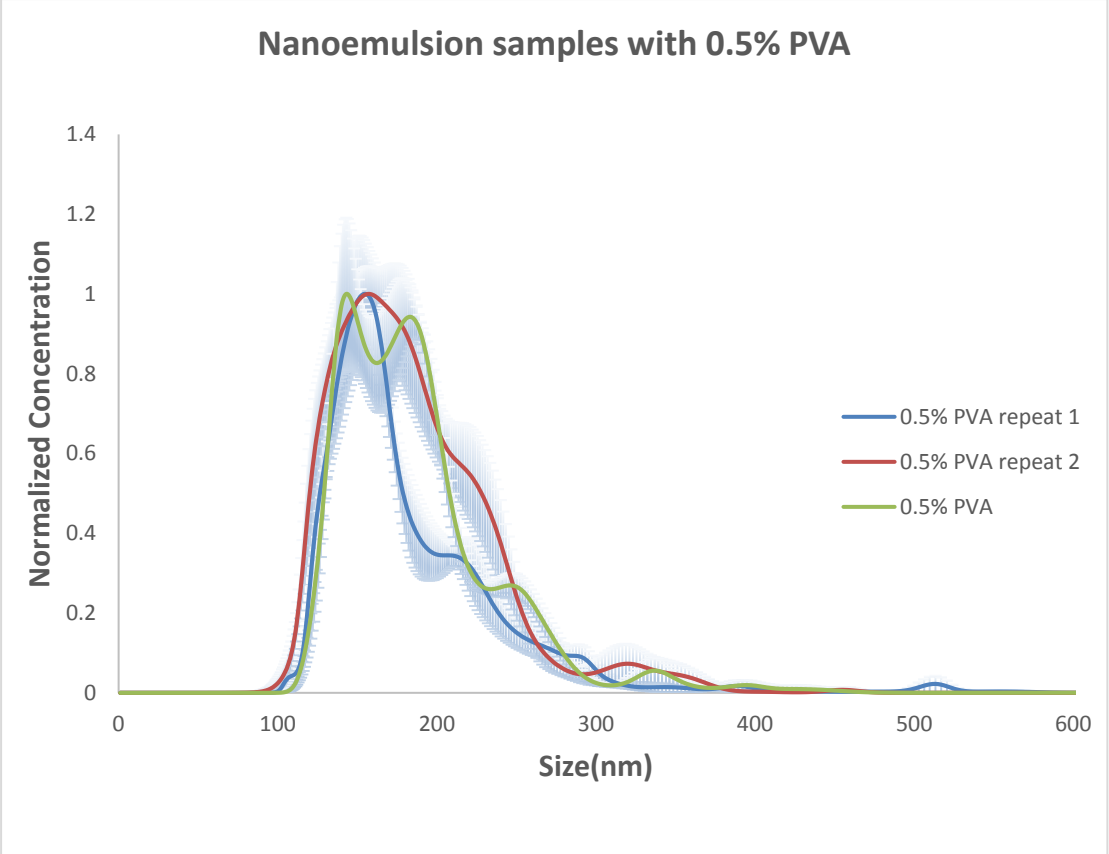

Figure 2.17 Emulsion sample with 0.5% PVA concentration.

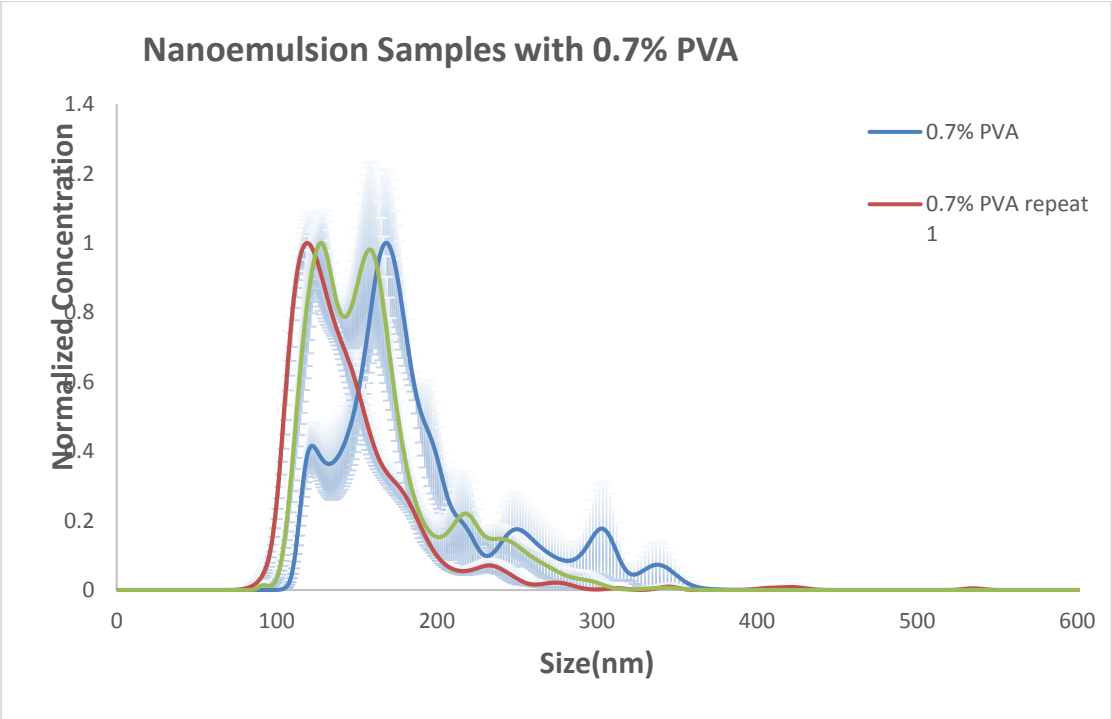

Figure 2.18 Emulsion sample with 0.7% PVA concentration.

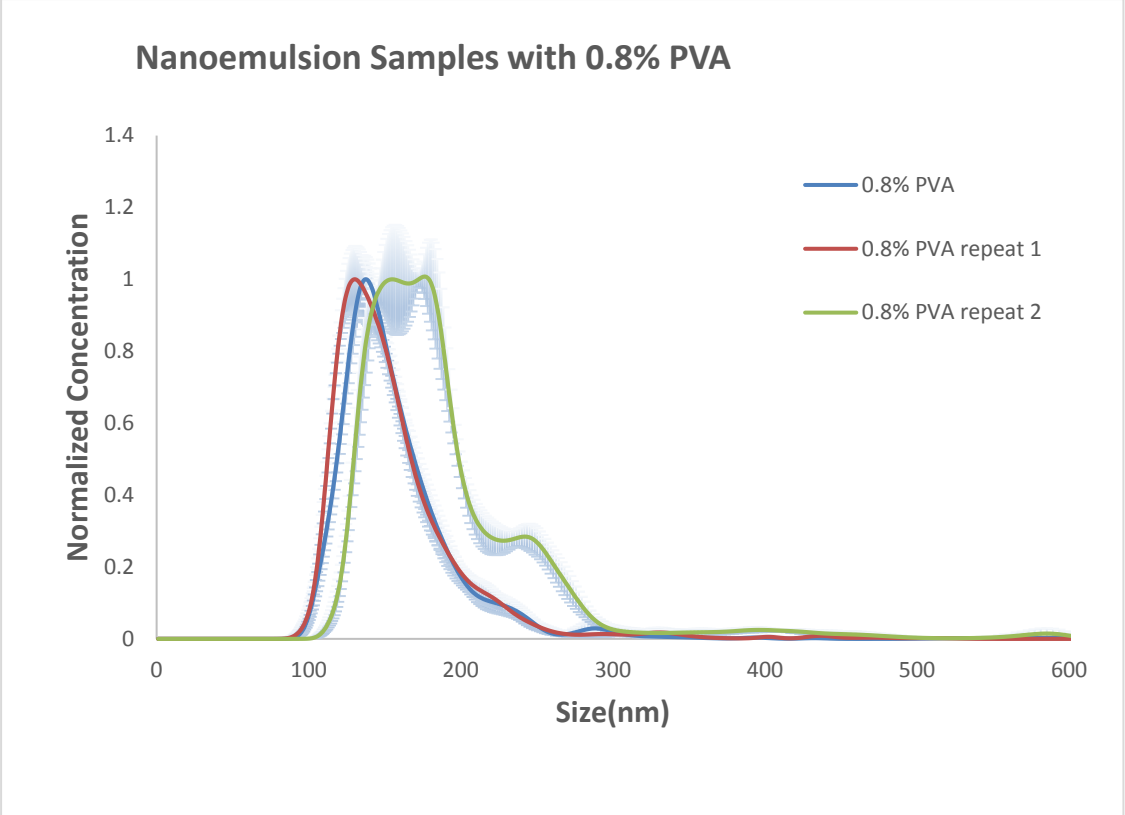

Figure 2.19 Emulsion sample with 0.8% PVA concentration.

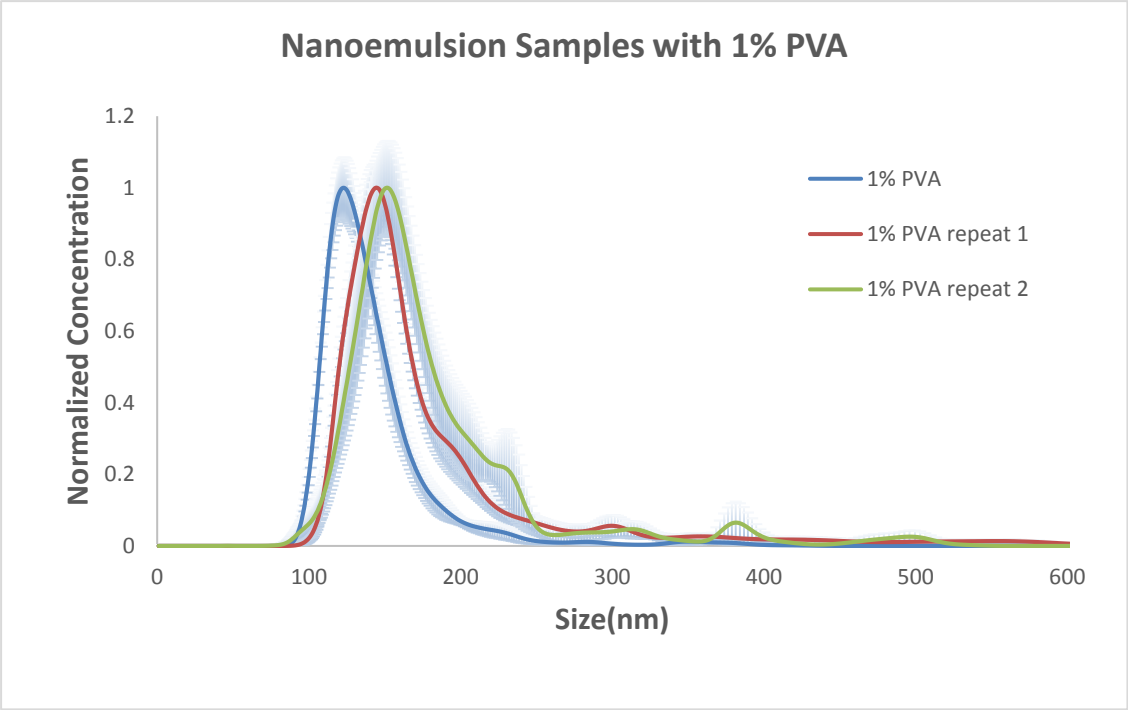

Figure 2.20 Emulsion sample with 1.0% PVA concentration.

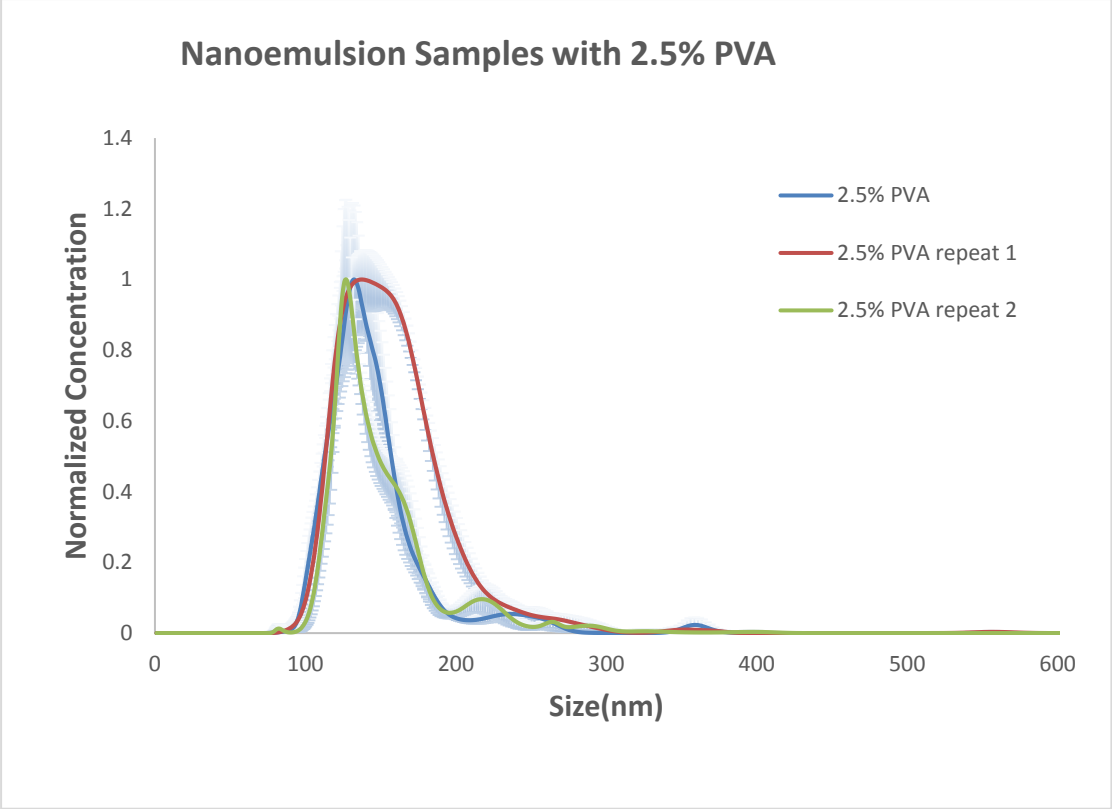

Figure 2.21 Emulsion sample with 2.5% PVA concentration.

Samples with 0.5% PVA concentration have a wide particle size range from 100 to 300 nm. Samples with 0.7% PVA concentration have a slightly smaller average size with the majority of particles within the 100 to 300 nm range. 0.8% PVA concentration leads to a significant decrease with most of nanoparticles within the 100 to 200 nm range. Small peaks within the 200 to 250 nm range were observed. Samples with 1% and 2.5% PVA have almost the same size distribution.

It can be observed that the PVA effects reached a maximum after reaching 2.5% PVA concentration. Due to the lack of samples of PVA concentration between 1% and 2.5% percent and above 2.5%, it is still not sure if the size can be further decreased between that range.

The mode and mean size, reported in the table below, both decrease when the PVA concentration increases from 0.5% to 2.5%. Samples with 1% PVA have almost the same mode and mean size with 0.7% PVA samples, while the 0.8% samples look slightly larger.

Table 1.3 Nanoemulsion PVA Concentration Effect on Size with Standard Error.

PVA Concentration	**Mode Size(nm)**	**Mean Size(nm)**
0.5%	172.6 +/- 8.3	178.3 +/- 2.9
0.5% repeat 1	156.3+/-6.8	171.3+/-2.5
0.5% repeat 2	159.9+/-7.0	173.3+/-2.0
0.7%	170.0+/-7.2	175.3+/-2.2
0.7% repeat 1	117.5 +/- 2.1	137.4 +/- 0.7
0.7% repeat 2	137.5+/-8.2	152.4+/-1.5
0.8%	138.2 +/- 1.9	150.8 +/- 1.4
0.8% repeat 1	136.2 +/- 4.0	147.6 +/- 1.1
0.8% repeat 2	168.6 +/- 5.2	177.9 +/- 1.7
1%	123.1 +/- 2.0	135.5 +/- 1.2
1% repeat 1	144.9 +/- 2.3	162.8 +/- 2.4
1% repeat 2	148.5 +/- 3.9	167.6 +/- 5.6
2.5%	136.4 +/- 5.0	140.0 +/- 2.8
2.5% repeat 1	134.8 +/- 4.3	151.2 +/- 2.3
2.5% repeat 2	128.8 +/- 2.2	143.7 +/- 2.3

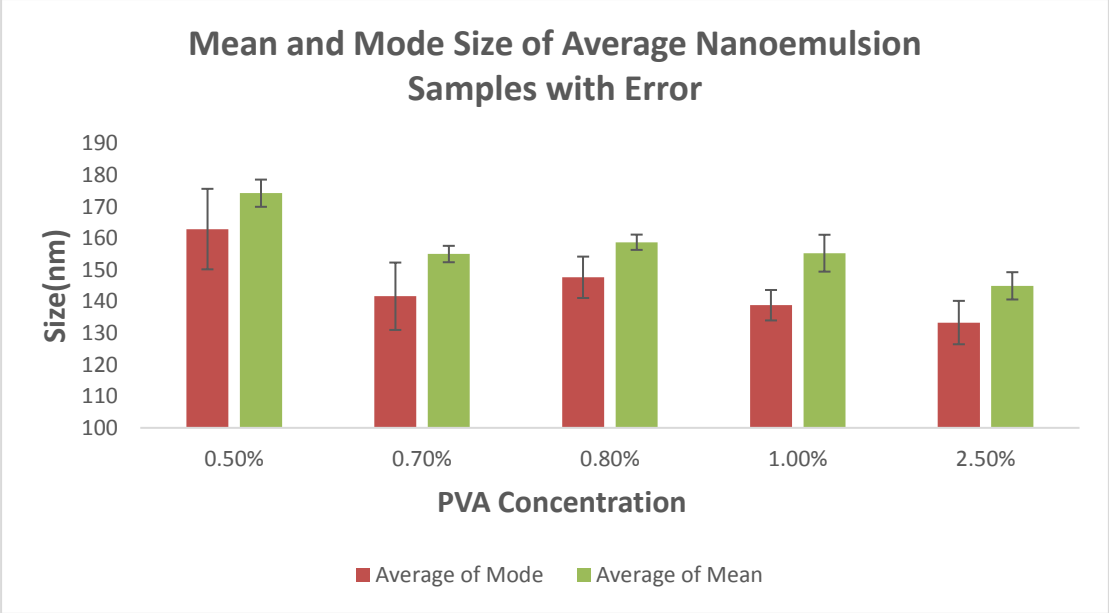

Figure 2.22 Nanoemulsion Average Samples Mode and Mean Size with Error.

Table 1.4 Average Mode and Mean of Nanoemulsion Samples with Standard Error (Unit. nm)

PVA Concentration	Average of Mode	Average of Mean	Standard Error	Standard Error of Mean
0.50%	162.93	174.30	12.75	4.31
0.70%	141.67	155.03	10.67	2.60
0.80%	147.67	158.77	6.55	2.42
1.00%	138.83	155.30	4.82	5.84
2.50%	133.33	144.97	6.87	4.32

2.11 Effect of PVA Concentration on Nanoprecipitation

Samples were made by nanoprecipitation with different PVA concentration and the resulting size and size distribution is reported below. These samples will be tested by DSC in the future. The PVA concentration ranges from 0.2% to 2.5%, while other variables remained same.

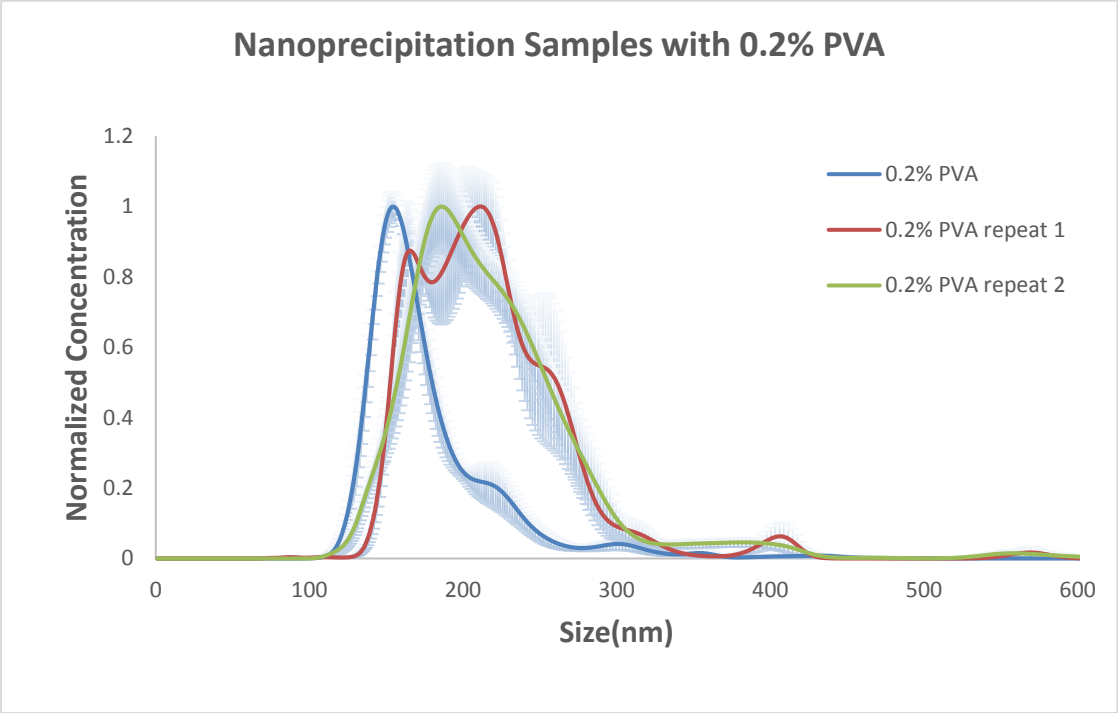

Figure 2.23 Nanoprecipitation sample with 0.2% PVA concentration.

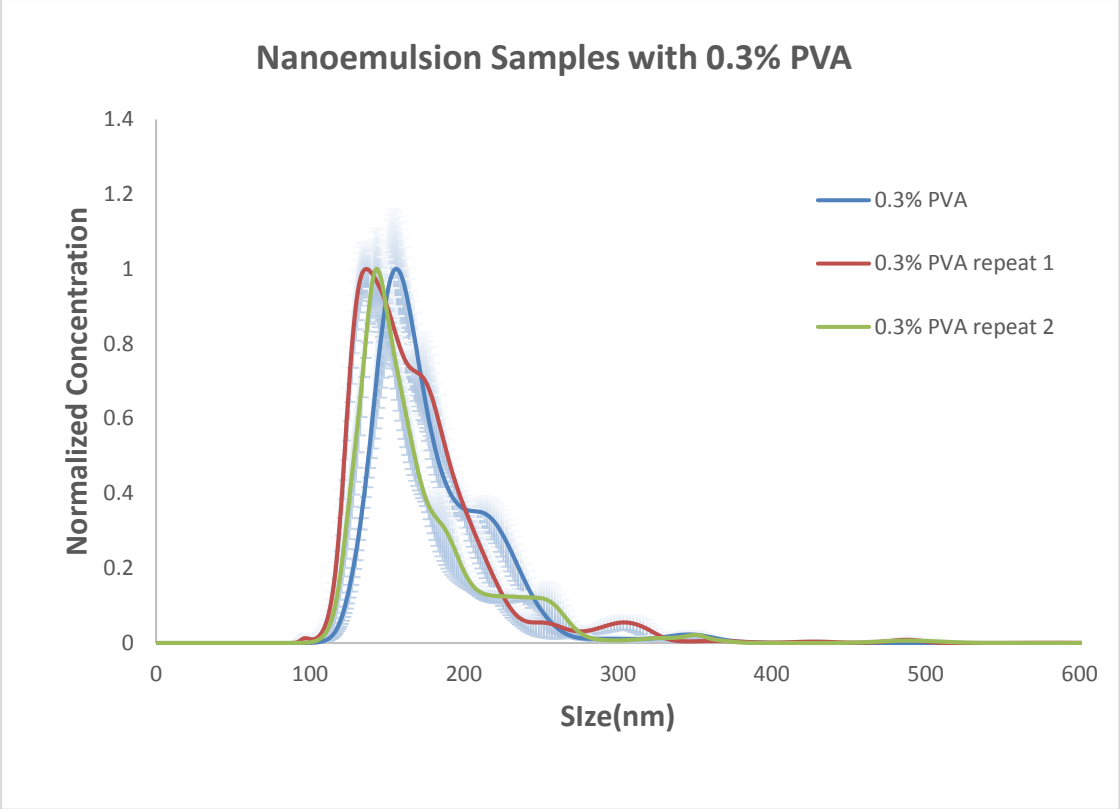

Figure 2.24 Nanoprecipitation sample with 0.3% PVA concentration.

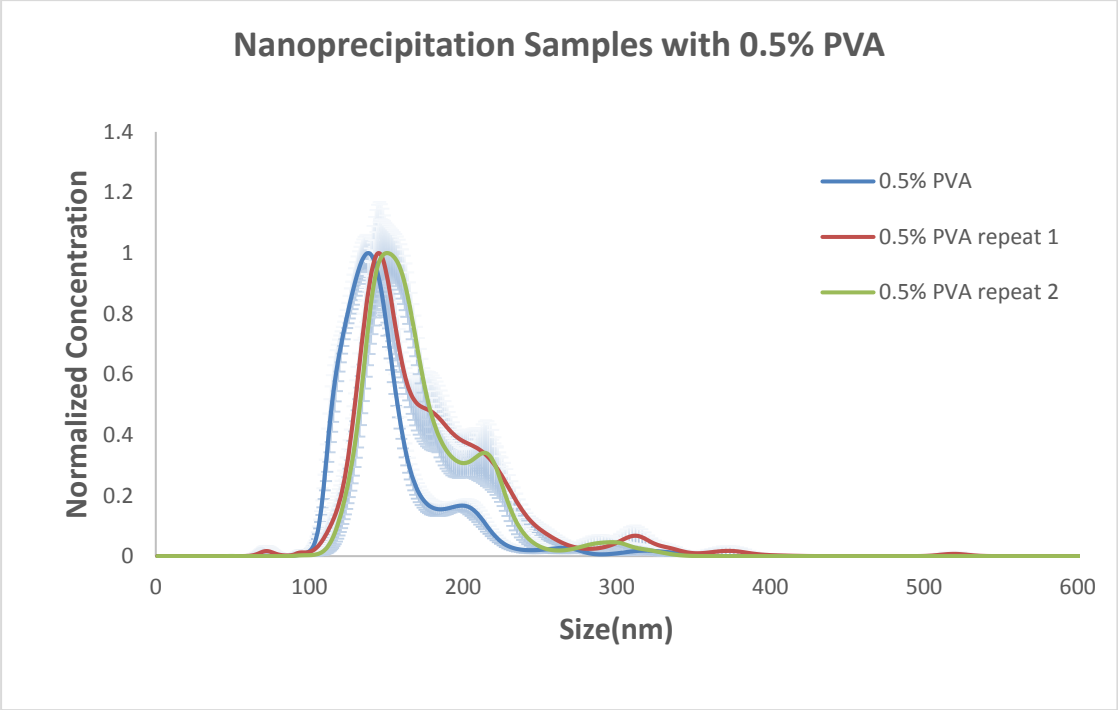

Figure 2.25 Nanoprecipitation sample with 0.5% PVA concentration.

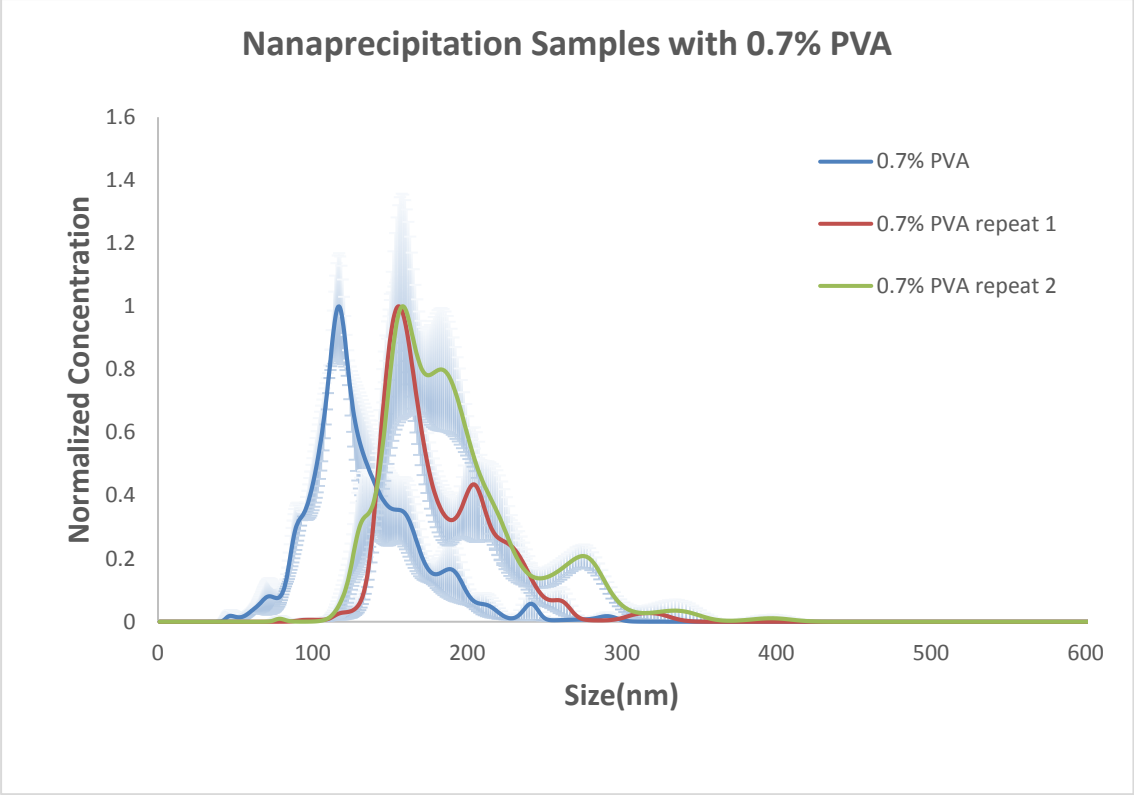

Figure 2.26 Nanoprecipitation sample with 0.7% PVA concentration.

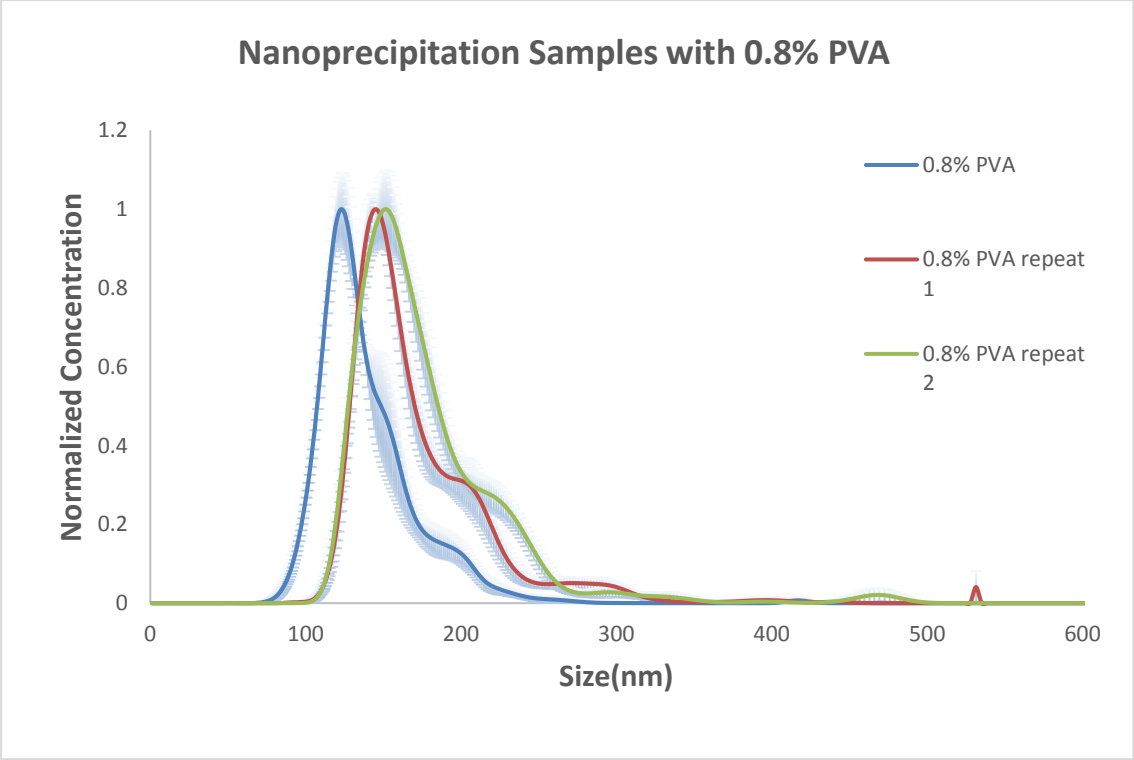

Figure 2.27 Nanoprecipitation sample with 0.8% PVA concentration.

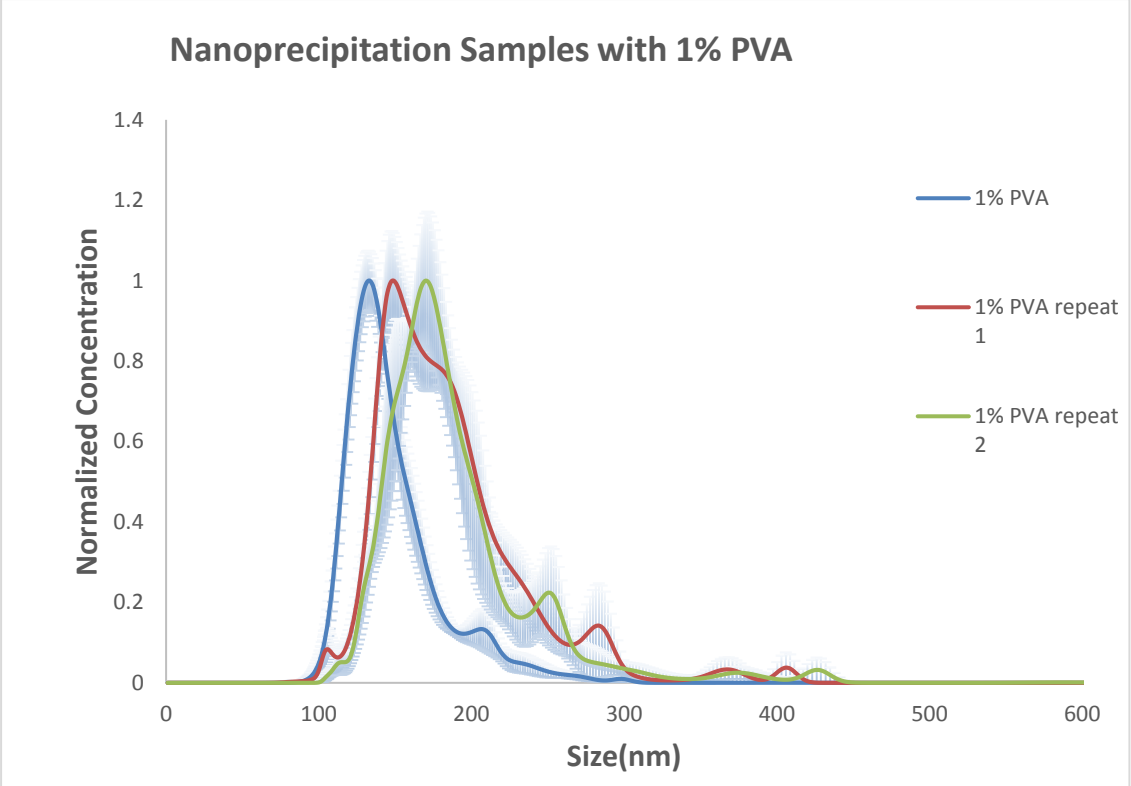

Figure 2.28 Nanoprecipitation sample with 1.0% PVA concentration.

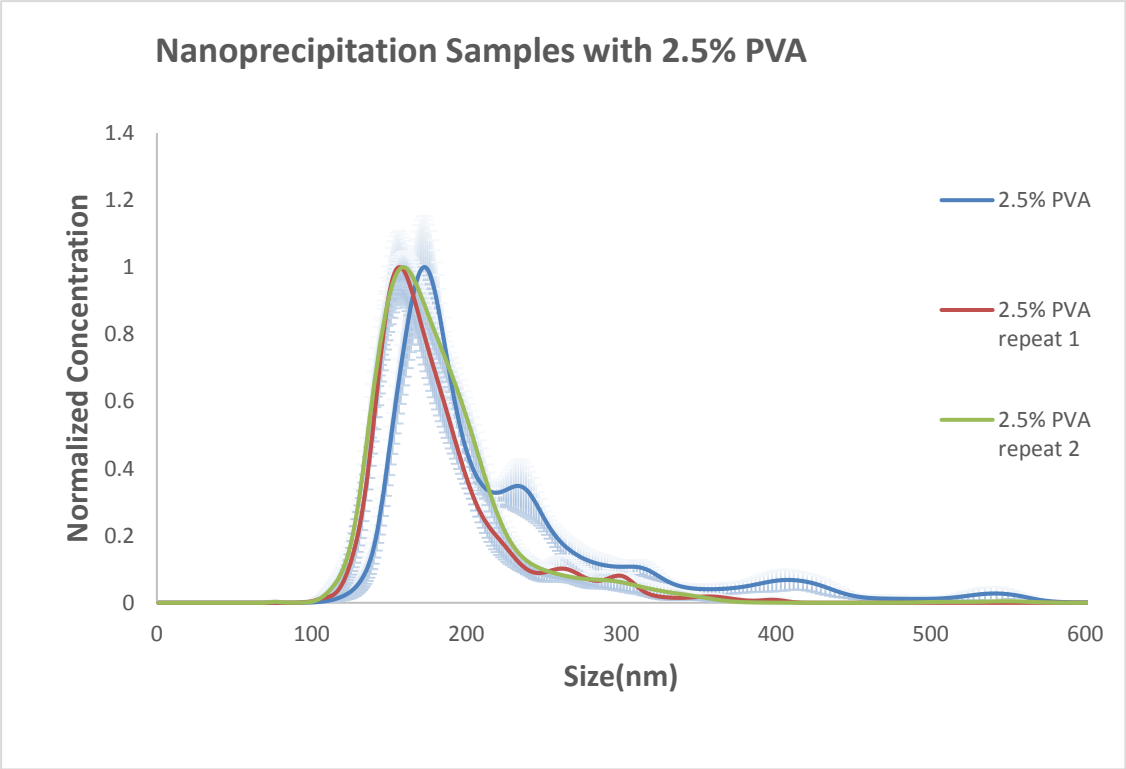

Figure 2.29 Nanoprecipitation sample with 2.5% PVA concentration.

Samples with 0.2% PVA concentration have poor size distribution and the sizes range from 100 to 300 nm with many peaks. Samples with 0.3% PVA look slightly better with sizes between 100 and 250 nm and fewer peaks. 0.5% samples have no difference compared to 0.3% PVA samples. 0.7% PVA samples have several peaks in their size distribution. 0.8% PVA samples have a mode size around 150 nm while the size span remains the same as with 0.7% PVA samples. 1.0% PVA samples and 2.5% PVA samples have an increase in mode and mean size as observed from the table below. The size decreased as the PVA concentration increased to around 0.5% PVA. Then, the size started to increase after at higher PVA concentrations. An increase in both mode and mean size were also observed. From the literature, it is well researched that when the PVA concentration reaches a certain point, the particle size will reach a minimum and further increase of PVA will increase the nanoparticle size instead. That is why we want to set different PVA concentration to observe this trend for a better size optimization. Due to lack of sample of PVA concentration between 1% and 2.5%, it remains unknown about how the size would change between those concentrations. Future work will include this. All the samples listed will be tested under TMDSC in the future.

Table 1.5 Nanoprecipitation PVA Concentration Effect on Size with Standard Error

PVA Concentration	**Mode Size(nm)**	**Mean Size(nm)**
0.2%	156.7 +/- 2.6	170.8 +/- 2.5
0.2% repeat 1	186.5 +/- 9.9	205.8 +/- 3.4
0.2% repeat 2	191.6 +/- 8.2	207.4 +/- 2.9
0.3%	160.1 +/- 3.7	172.3 +/- 0.7
0.3% repeat 1	138.6 +/- 3.6	161.4 +/- 1.7
0.3% repeat 2	146.2 +/- 3.2	162.6 +/- 2.9
0.5%	136.4 +/- 2.5	145.1 +/- 1.1
0.5% repeat 1	150.6 +/- 7.1	167.9 +/- 1.7
0.5% repeat 2	152.7 +/- 3.4	166.2 +/- 1.3
0.7%	118.1 +/- 2.1	123.6 +/- 1.1
0.7% repeat 1	156.3 +/- 3.0	175.4 +/- 2.6
0.7% repeat 2	170.8 +/- 7.6	181.8 +/- 0.9
0.8%	129.8 +/- 4.8	137.3 +/- 3.7
0.8% repeat 1	146.8 +/- 2.3	163.4 +/- 2.4
0.8% repeat 2	149.1 +/- 4.0	167.4 +/- 1.7
1%	133.5 +/- 2.2	143.4 +/- 2.0
1% repeat 1	160.8 +/- 7.9	175.3 +/- 2.1
1% repeat 2	169.8 +/- 6.8	179.8 +/- 1.7
2.5%	170.7 +/- 3.7	204.6 +/- 5.1
2.5% repeat 1	157.2 +/- 1.7	174.6 +/- 1.8
2.5% repeat 2	158.7 +/- 3.0	175.1 +/- 1.7

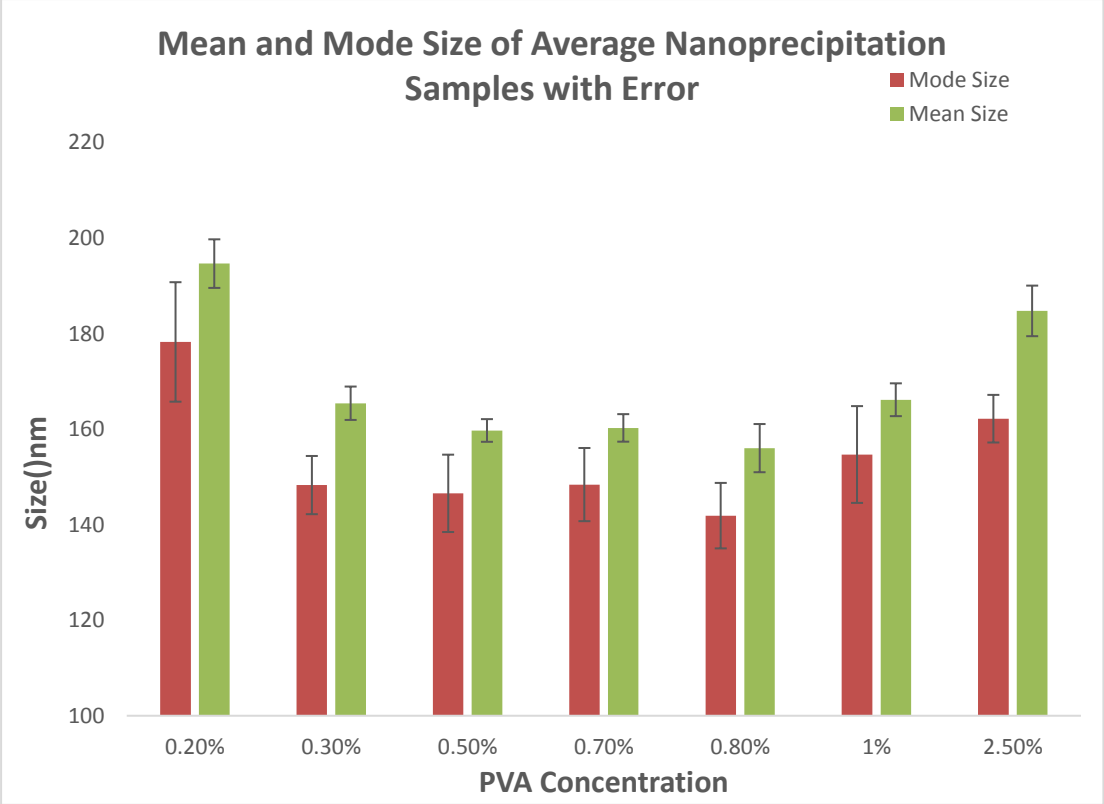

Figure 2.30 Average of Repeat Samples on Mode and Mean size versus PVA Concentration.

Table 1.6 Average Mode and Mean of Nanoprecipitation Samples with Standard Error (Unit. nm)

PVA Concentration	Average of Mode	Average of Mean(	Standard Error of Mode	Standard Error of Mean
0.20%	178.27	194.67	12.51	5.09
0.30%	148.30	165.43	6.09	3.49
0.50%	146.57	159.73	8.10	2.38
0.70%	148.40	160.27	7.66	2.88
0.80%	141.90	156.03	6.85	5.04
1.00%	154.70	166.17	10.13	3.44
2.50%	162.20	184.77	4.98	5.30

It is obvious that even with the same methods, the size can fluctuate a bit. The difference between the maximum size and the minimum size can be 30 nm. So, the statistical analysis of a one-way ANOVA was performed with a Tukey test to determine

the significant difference between groups. The results show that the mode size of nanoemulsion samples of 0.5% PVA concentration is significantly different from the other samples. The 0.8% and 2.5% samples are also significantly different from each other, while the 1% and 0.7% samples are not significantly different. Though the mean size of nanoemulsions only shows a significant difference on 0.5% to 0.7%, 1% and 2.5% samples, and 0.7%, the 1% and 2.5% samples are not significantly different. The results also show that the mode size of nanoprecipitation samples with 0.2% PVA concentration is significantly different from other samples except 2.5% samples. 2.5% samples are also different from other samples except 0.2% samples, while 0.3%, 0.5%, 0.7%, 0.8% and 1% samples are of no significant differences. The results of the statistical analysis of the mean size of nanoprecipitation particles only shows significant differences between 0.2% and other samples except 2.5% samples. The other samples are not significantly different.

Particles made from nanoprecipitation and nanoemulsion with similar size can be compared with each other as the samples of same size nanoparticles made from different methods with different thermal history using DSC.

Nanoprecipitation samples above 0.7% PVA concentration have a size range between 100 and 200 nm. Nanoprecipitation samples above 0.5% PVA concentration also have a size range between 100 and 200 nm. Thus these samples can be used for DSC testing and they are suitable samples with almost the same size distribution but of different thermal history. They will be tested under DSC in the future.

2.12 DSC Procedure

The samples were sealed inside the DSC pans with lids using a pan press. An empty reference pan was made and sealed as well. Both the sample pan and the reference pan were weighted and placed inside the DSC chamber. The average heating rate was 1°C/min and the amplitude was 1°C. The period was set at 40 seconds. The temperature was increased from 20°C to 80°C, followed by holding at 80°C for 2 min. Then, the samples were cooled down at a rate of 1°C /min to 20°C. Then, they were held isothermally at 20°C for 2 minutes. Then samples were heated again at the rate of 1°C /min to 80°C.

Due to limited access to an appropriate DSC, only preliminary data has been collected. The samples that were run on the DSC were made early in the project and the sample procedure varied slightly from previously discussed samples. For the nanoprecipitation recipes, 0.1% PVA was dissolved in 100 ml water and 20 to 25 mg of PLGA was dissolved inside 2 ml of acetone. For the sample made with salt, sodium chloride was dissolved in the aqueous solution to make a 50 mmol/L salt solution in order to increase the ionic strength to increase the particle size. For the sample made with double the concentration (double organic phase concentration), the amount of PLGA was increased to 45 to 50 mg. In these early samples the PVA was not properly dissolved. Thus, the actual PVA concentration is actually lower than 0.1%. For the nanoemulsion recipes, 0.5% PVA was dissolved in 4 ml water. 20 to 25 mg of PLGA was dissolved inside 1 ml of chloroform. Again, PVA was not properly dissolved and the actual PVA concentration should be around 0.7% which can be concluded from previous size tuning experiments. 1 ml of the PLGA in chloroform solution was injected into the PVA solution. The sample was sonicated using an amplitude of 80 (around 17 J energy) for 1 min for the 1 min sample and 10 min for the 10 min sample. The rest of

the procedures remain the same for all of the nanoprecipitation and nanoemulsion samples.

2.13 DSC Data Analysis

Below are the TMDSC results of the PLGA samples. The blue line represents the first heating scan. The purple line that overlaps the blue one represents the second heating scan. The red line at the top of the graph represents the first cooling scan. They are all the reversing flow data. The total heat flow and non-reversing flow have been excluded from the image. For the nanoprecipitation sample with 0.1% PVA concentration, the cooling process was not recorded.

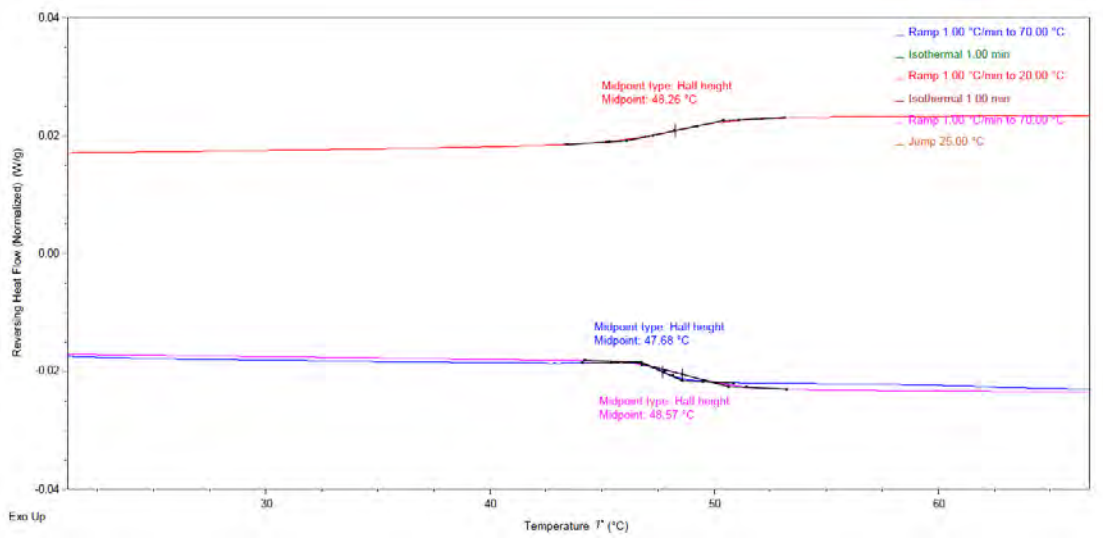

Figure 2.31 PLGA bulk from bottle.

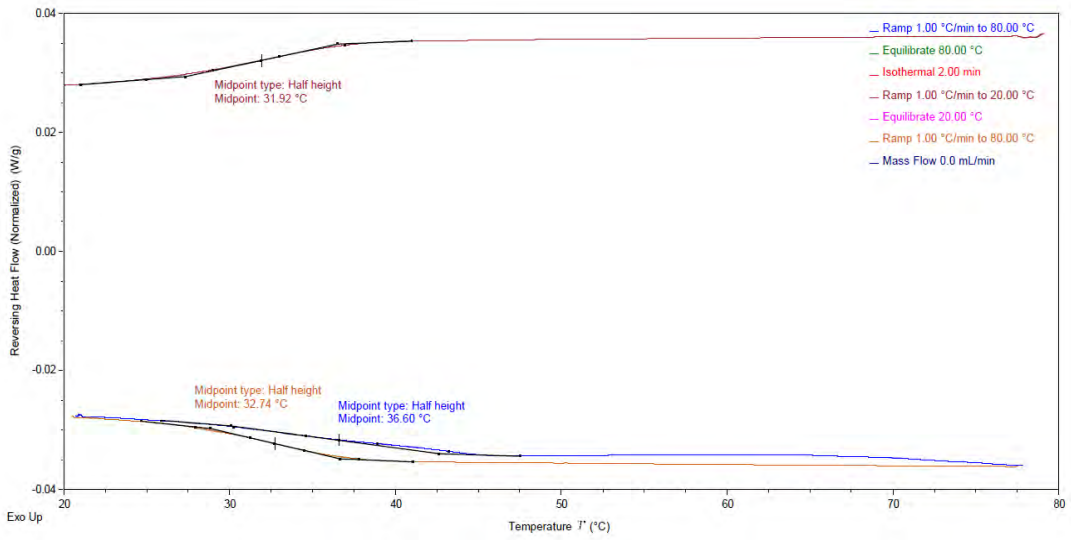

Figure 2.32 Nanoprecipitation sample with 0.1% PVA concentration.

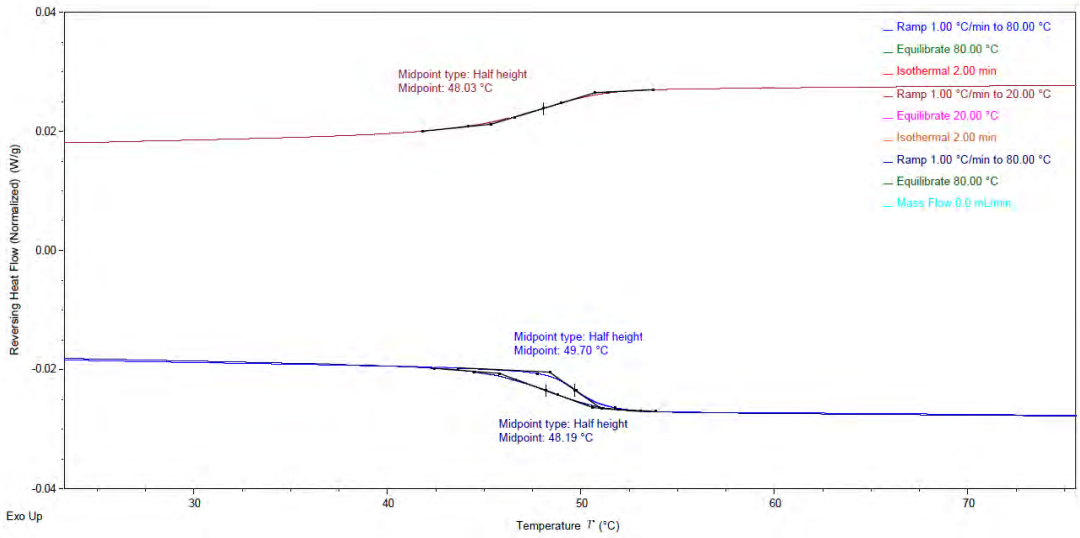

Figure 2.33 1min sonication.

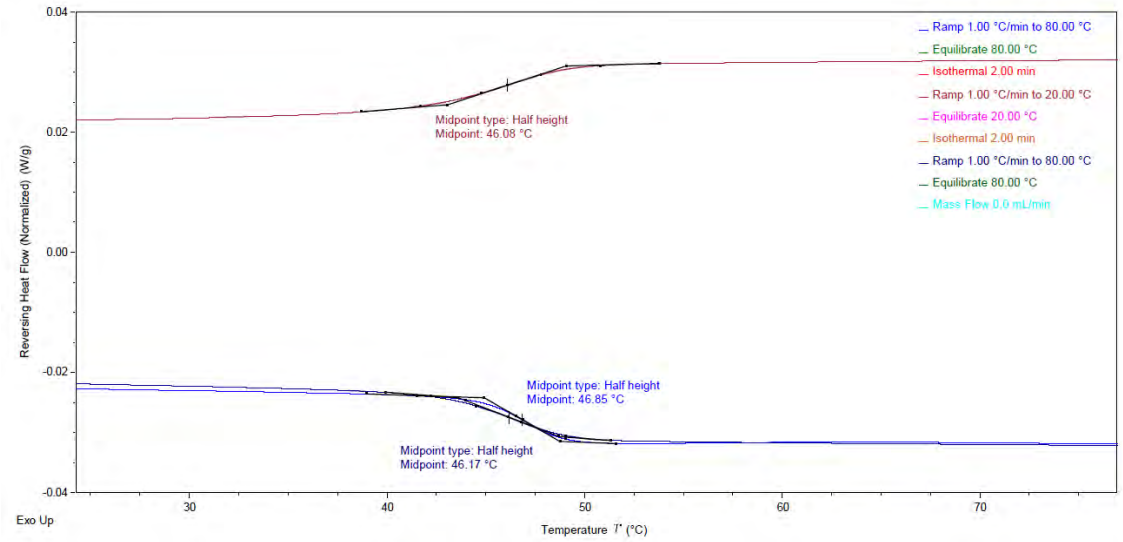

Figure 2.34 10min sonication.

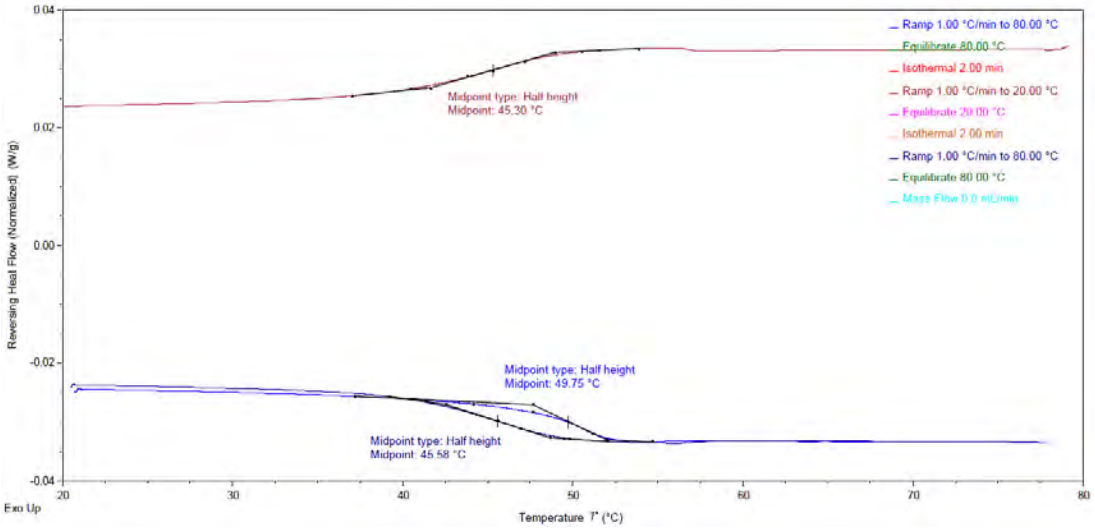

Figure 2.35 50mM salt nanoprecipitation.

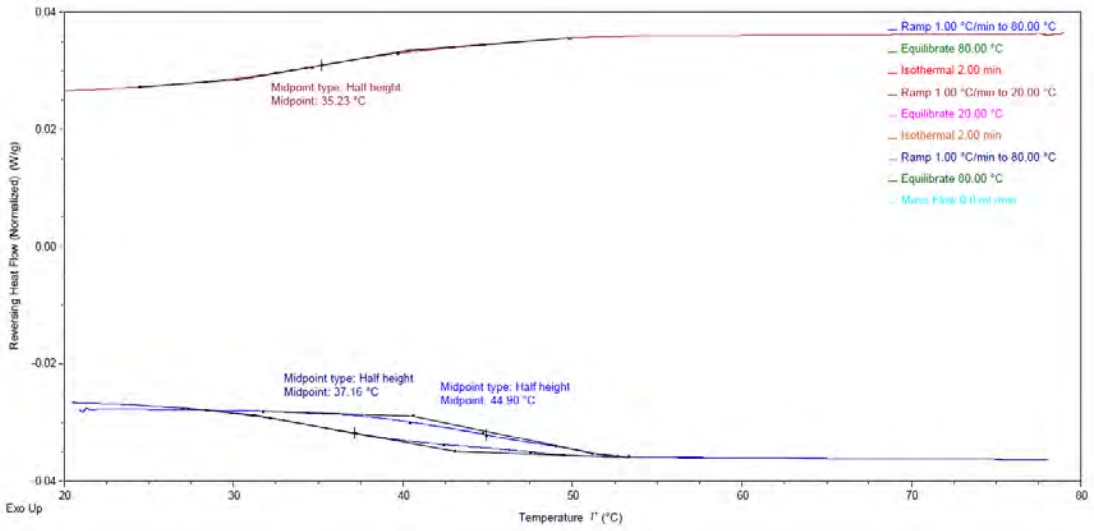

Figure 2.36 Double PLGA organic phase concentration nanoprecipitation.

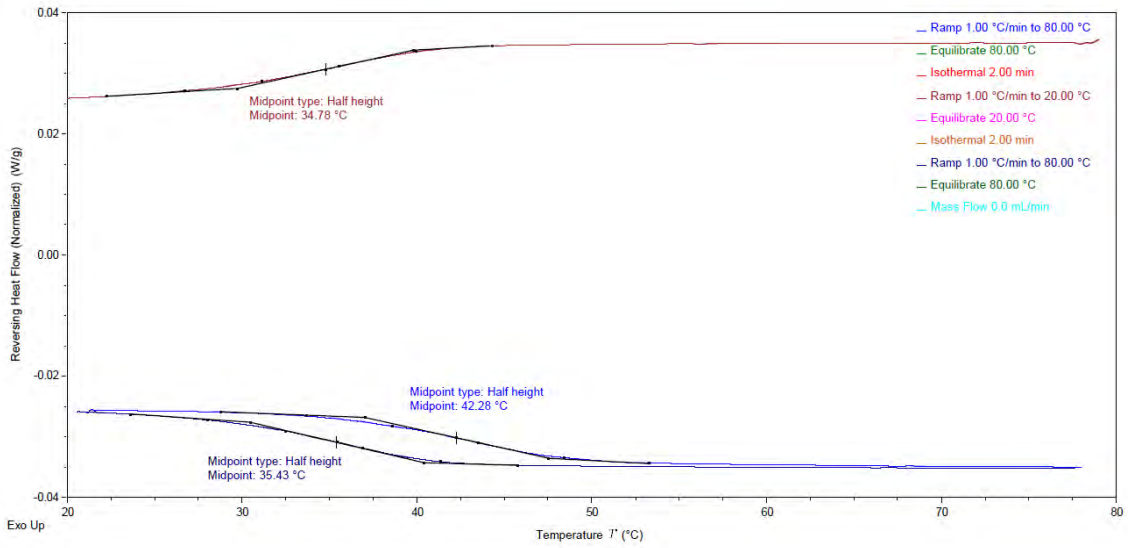

Figure 2.37 Double PLGA organic phase concentration nanoprecipitation repeat 1.

The results of TMDSC is displayed above and show that we are getting clear measurements of Tg from the first heating scan. TMDSC is a viable way to study the effect of thermal history on the Tg. The non-reversing flow and total heat flow were not displayed here. It can be observed that PLGA samples' bulk Tg is around 48°C. The first heating Tg, second heating Tg and the first cooling Tg value of PLGA bulk are relatively close. In several of the samples, particularly the nanoprecipitation samples, the Tg on the second heating scan is still very different from that of the bulk. This could suggest that the samples have only partially relaxed and the thermal history has not been fully erased. The samples were only heated up to 80°C so for future experiments, the samples will be taken to higher temperatures and kept isothermal for a period to fully erase the thermal history.

Both nanoemulsion samples (1 min and 10 min samples) have their second heating Tg and first cooling Tg very close to the first heating Tg. They also are closer to the bulk Tg value than the nanoprecipitation samples.

The table including the Tg of first heating, first cooling and second heating is displayed below. It shows a trend that the nanoprecipitation samples have a wider Tg span than nanoemulsion and bulk samples. The Tg span of the nanoprecipitation samples is around 9°C, while the Tg span of the nanoemulsion samples is about 4°C. This trend can be observed on all three heating and cooling Tg. Further samples will be tested to make sure if this trend is consistent in the future.

Table 1.7 TMDSC Tg Results

TMDSC Tg Results						
Samples' name	First heating Tg(°C)	Second Heating Tg(°C)	First cooling Tg(°C)	First heating Tg (°C) span	ΔT of 1st heating Tg with bulk's 2nd heating Tg (°C)	ΔT of 1st heating Tg with 2nd heating Tg (°C)
PLGA bulk	47.68	48.57	48.26	2	NA	-0.89
Nanoprecipitation 0.1% PVA	36.6	32.74	31.92	11.16	-11.97	3.86
Nanoprecipitation 50 mM salt 0.1% PVA	49.75	45.58	45.30	3.74	1.18	4.17
Nanoprecipitation double organic phase 0.1% PVA	44.90	37.16	35.23	11.4	-3.67	7.74
Nanoprecipitation double organic phase 0.1% PVA repeat sample	42.28	35.43	34.78	10.05	-4.29	8.85
Nanoemulsion 1min	49.70	48.19	48.03	2.6	1.13	1.51
Nanoemulsion 10 min	46.85	46.17	46.08	4.02	-1.72	0.68

Several samples were sent to TA Instruments for testing and the results are below. However, they used a different heating and cooling rate of 3°C /min. The Tg will change depending on the speed used to probe it so the resulting Tg values from this data cannot be compared to the previous data collected at a different scan rate.

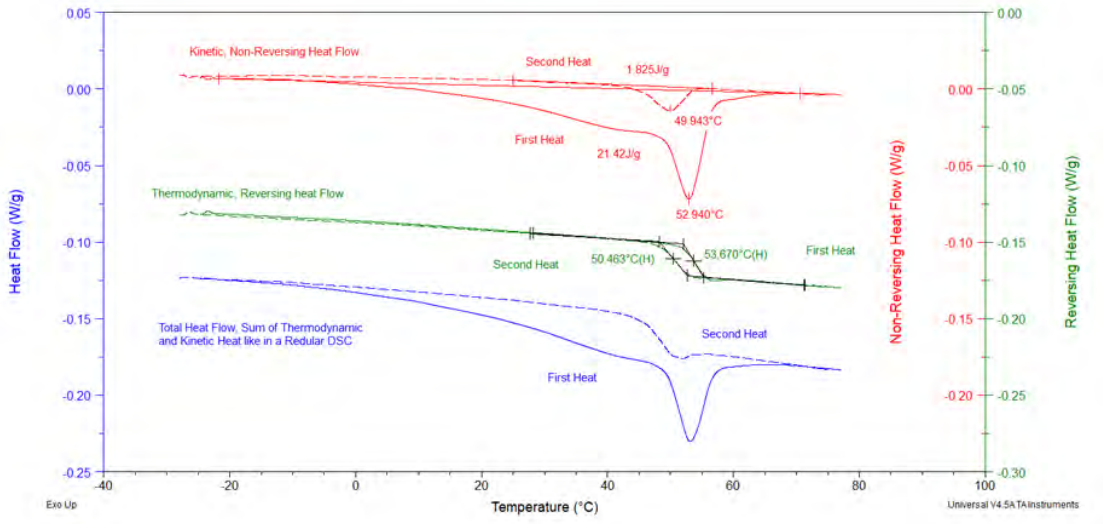

Figure 2.38 Nanoprecipitation with 0.5% PVA concentration.

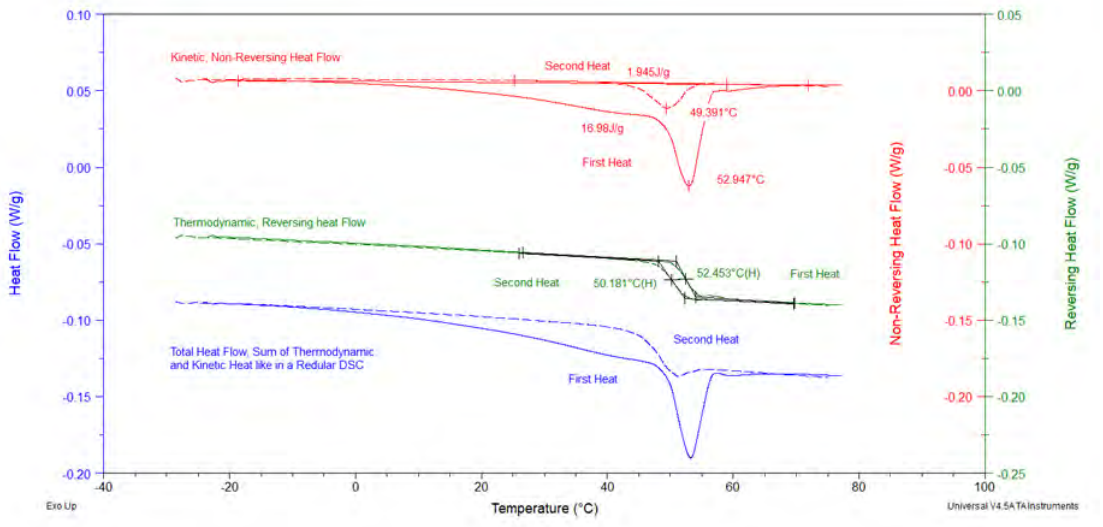

Figure 2.39 Nanoprecipitation with 0.5% PVA concentration same sample retest.

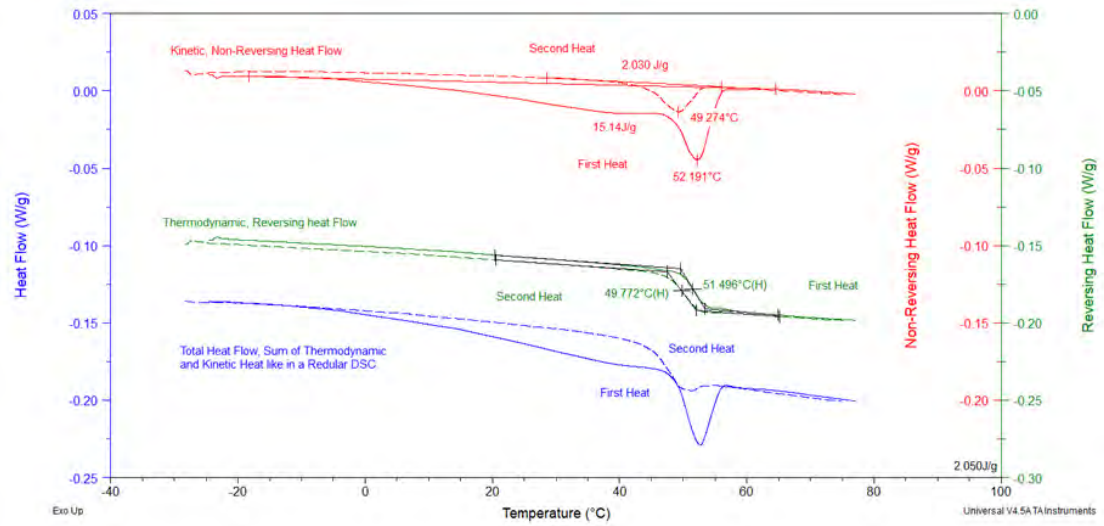

Figure 2.40 Nanoemulsion with 1 min sonication.

It can be observed that the nanoprecipitation has Tg at around 52 and 53 °C, while the Tg of nanoemulsion at around 51 °C. We can't get much information from these samples unless we get more samples tested by the same heating and cooling rate. Worth noting though is the accuracy of the results from the two runs of sample from the same batch. The Tg values only vary by about 1°C or less for these samples. Although more runs would be needed to confirm the accuracy of these results, this preliminary data is promising.

CHAPTER 3

FUTURE WORK

More PVA gradients between 1% and 2.5% and above 2.5% percent might be studied if needed in the future. NTA data of electrospray jetting will be collected in the future. Further stability in electrospray jetting can be achieved by using triple voltage methods to modulate and control the morphology and size of nanoparticles. and might be done in the future. Samples of nanoemulsion, nanoprecipitation and electrospray jetting will be tested by DSC with an improved protocol. Samples will be kept isothermal at 20°C for 5 mins and then heated up to 80°C with 1°C/min average rate with an amplitude of 1°C and a 60 s period of modulated temperature. The sample will be kept isothermal at 80°C for 5 min and then cooled down with the same speed and temperature modulation. Once it reaches 20°C, the sample will be kept isothermal for 5 min, then will be heated up to 190°C and kept isothermal for 10 min to make sure the thermal history is entirely erased. Then, the sample will be cooled down to 20°C at the same speed and kept isothermal for 5 min. Then, the sample will be heated again to 80°C. This improved protocol will allow the acquisition of three heating Tg's and 2 cooling Tg's which would be very helpful on data analysis. The effect of thermal history on drug release of PLGA nanoparticles will be researched in the future. A drug release study will be done using Rhodamine B as drug substitute. It was investigated that the Tg can affect drug release behavior. We hypothesize that thermal history, which has effect on Tg, will influence drug release behavior.

APPENDIX A

NTA SAMPLE TABLE

Table A.1 to A.2 show mode and mean size of PLGA nanoparticles.

Table A.1 Nanoemulsion PVA concentration effect on size

Nanoemulsion PVA concentration effect on size		
PVA Concentration	Mode Size(nm)	Mean Size(nm)
0.5%	143.4	177.9
0.5% repeat 1	154.8	171.6
0.5% repeat 2	157.2	173.6
0.7%	165.7	175.7
0.7% repeat 1	119.0	137.3
0.7% repeat 2	127.6	152.3
0.8%	137.6	150.6
0.8% repeat 1	130.3	147.5
0.8% repeat 2	176.2	177.9
1%	122.9	135.6
1% repeat 1	144.6	163.4
1% repeat 2	151.6	166.8
2.5%	132.3	139.8
2.5% repeat 1	137.5	151.1
2.5% repeat 2	126.9	143.9

Table A.2 Nanoprecipitation PVA concentration effect on size

Nanoprecipitation PVA concentration effect on size		
PVA Concentration	Mode Size(nm)	Mean Size(nm)
0.2%	152.7	166.1
0.2% repeat 1	211.3	206.9
0.2% repeat 2	186.1	207.4
0.3%	156.1	172.4
0.3% repeat 1	136.6	161.4
0.3% repeat 2	143.4	162.4
0.5%	138.3	145.1
0.5% repeat 1	145.1	168.9
0.5% repeat 2	150.6	166.2
0.7%	118.7	123.5
0.7% repeat 1	155.7	175.3
0.7% repeat 2	158.3	182.0
0.8%	124.1	138.2
0.8% repeat 1	145.1	163.4
0.8% repeat 2	151.5	167.3
1%	136.8	152.6
1% repeat 1	148.6	175.1
1% repeat 2	170.3	180.0
2.5%	172.9	204.3
2.5% repeat 1	156.9	175.0
2.5% repeat 2	159.3	175.2

APPENDIX B

DSC RESULTS TABLE

Table B.1 to B.2 show DSC data results.

Table B.1 TMDSC Tg Results

TMDSC Tg Results						
Samples	First heating Tg	Second Heating Tg	First cooling Tg	Difference of first heating Tg with PLGA bulk	Difference of second heating Tg with PLGA bulk	Difference of first cooling Tg with PLGA bulk
PLGA bulk	47.68	48.57	48.26	NA	NA	NA
Nanoprecipitation 0.1% PVA	36.6	32.74	31.92	11.08	15.83	16.34
Nanoprecipitation 50 mM salt 0.1% PVA	49.75	45.58	45.30	2.07	2.99	2.96
Nanoprecipitation double organic phase 0.1% PVA	44.90	37.16	35.23	2.79	11.41	13.03

Nanoprecipitation double organic phase 0.1% PVA repeat sample	42.28	35.43	34.78	3.4	13.16	13.48
Nanoemulsion 1min	49.70	48.19	48.03	2.02	0.38	0.23
Nanoemulsion 10 min	46.85	46.17	46.08	0.83	2.4	2.18

Table B.2 TMDSC Tg Results Continued

TMDSC Tg Results Continued						
Samples	First heating Tg	Second Heating Tg	First cooling Tg	First heating Tg span	Second heating Tg span	First cooling Tg span
PLGA bulk	47.68	48.57	48.26	46.69 ~48.69	46.52 ~50.61	45.85 ~50.19
Nanoprecipitation 0.1% PVA	36.6	32.74	31.92	29.41 ~40.57	28.53 ~37.16	27.44 ~35.97
Nanoprecipitation 50 mM salt 0.1% PVA	49.75	45.58	45.30	48.23 ~51.97	42.58 ~49.13	42.42 ~48.91
Nanoprecipitation double organic phase 0.1% PVA	44.90	37.16	35.23	40.44 ~51.84	31.25 ~42.09	29.6 ~41.5

Nanoprecipitation double organic phase 0.1% PVA repeat sample	42.28	35.43	34.78	37.67 ~47.72	30.31 ~39.74	29.82 ~39.87
Nanoemulsion 1min	49.70	48.19	48.03	48.4 ~51.0	46.1 ~50.76	45 ~50.5
Nanoemulsion 10 min	46.85	46.17	46.08	44.89 ~48.91	43.5 ~48.96	42.85 ~48.33

APPENDIX C

STATISTICAL ANALYSIS RESULTS

Table C.1 to C.4 show results of the one-way ANOVA with Tukey test of nanoprecipitation and nanoemulsion means and modes with varying PVA concentration. Means that do not share a letter are significantly different.

Table C.1 Nanoprecipitation Mode Size

Factor	N	Mean	Grouping		
0.2%	15	178.25	A		
2.5%	15	162.19	A	B	
1%	15	154.69		B	C
0.7%	14	150.18		B	C
0.3%	15	148.31		B	C
0.5%	15	142.83			C
0.8%	14	142.77		B	C

Table C.2 Nanoprecipitation Mean Size

Factor	N	Mean	Grouping		
0.2%	15	194.65	A		
2.5%	15	184.78	A	B	
1%	15	166.17		B	C
0.3%	15	165.43			C
0.7%	14	163.00			C
0.8%	14	156.33			C
0.5%	15	156.15			C

Table C.3 Nanoemulsion Mode Size

Factor	N	Mean	Grouping		
0.5%	15	162.97	A		
0.8%	15	147.65	A		B
0.7%	14	140.77			B
1%	15	138.84			B
2.5%	15	133.31			B

Table C.4 Nanoemulsion Mean Size

Factor	N	Mean	Grouping		
0.5%	15	174.30	A		
0.8%	15	158.73		B	
1%	15	155.31		B	C
0.7%	14	153.83		B	C
2.5%	15	144.97			C

REFERENCES

1. Makadia, H. K.; Siegel, S. J. *Polymers* **2011**, *3*(3), 1377–1397.

2. Bala, I.; Hariharan, S.; Kumar, M. R. *Crit Rev Ther Drug Carrier Syst* **2004**, *21*(5), 387–422.

3. Joy, J.; Thomas, S. *Nanoparticles in Polymer Systems for Biomedical Applications* **2018**, 23–56.

4. Alonso-Sande, M.; Rieux, A. D.; Fievez, V.; Sarmento, B.; Delgado, A.; Evora, C.; Remuñán-López, C.; Préat, V.; Alonso, M. J. *Biomacromolecules* **2013**, *14*(11), 4046–4052.

5. Ribeiro, S.; Hussain, N.; Florence, A. T. *Int. J. Pharm.* **2005**, *298*(2), 354–360.

6. Wang, Y.; Li, P.; Tran, T. T.-D.; Zhang, J.; Kong, L. *Nanomaterials* **2016**, *6*(2), 26.

7. Jonderian, A.; Maalouf, R. *Front Pharmacol* **2016**, *7*.

8. Swaminathan, S. K.; Roger, E.; Toti, U.; Niu, L.; Ohlfest, J. R.; Panyam, J. *J Control Release* **2013**, *171*(3), 280–287.

9. Sechi, M.; Sanna, V.; Pala, N. *Int J Nanomedicine* **2014**, 467.

10. Lee, S. H.; Zhang, Z.; Feng, S.-S. *Biomaterials* **2007**, *28*(11), 2041–2050.

11. Vettor, M.; Bourgeois, S.; Fessi, H.; Pelletier, J.; Perugini, P.; Pavanetto, F.; Bolzinger, M. A. *J. Microencapsul.* **2010**, *27*(3), 253–262.

12. Barreras-Urbina, C. G.; Ramírez-Wong, B.; López-Ahumada, G. A.; Burruel-Ibarra, S. E.; Martínez-Cruz, O.; Tapia-Hernández, J. A.; Félix, F. R. *INT J FOOD PROP* **2016**, *19*(9), 1912–1923.

13. Lappe, S.; Mulac, D.; Langer, K. *Int J Pharm* **2017**, *517*(1-2), 338–347.

14. Steendam, R.; Steenbergen, M. V.; Hennink, W.; Frijlink, H.; Lerk, C. *J Control Release* **2001**, *70*(1-2), 71–82.

15. Takeuchi, I. et al. *Colloids Surf A Physicochem Eng Asp* **2017**, 529, 328-333.

16. Park, P. I. P.; Jonnalagadda, S. *J. Appl. Polym. Sci.* **2006**, *100*(3), 1983–1987.

17. Khang, G.; Jeon, E. K.; Rhee, J. M.; Lee, I.; Lee, S. J.; Lee, H. B. *Macromol Res* **2003**, *11*(5), 334–340.

REFERENCES

(Continued)

18. Liu, Y.; Lu, Y. C.; Luo, G. S. *Soft Matter* **2014**, *10*(19), 3414.

19. Sah, E.; Sah, H. *J Nanomater* **2015**, *2015*, 1–22.

20. Miladi, K.; Sfar, S.; Fessi, H.; Elaissari, A. *Polymer Nanoparticles for Nanomedicines* **2016**, 17–53.

21. Anton, N.; Benoit, J.-P.; Saulnier, P. *J Control Release* **2008**, *128*(3), 185–199.

22. Bock, N.; Woodruff, M. A.; Hutmacher, D. W.; Dargaville, T. R. *Polymers* **2011**, *3*(1), 131–149.

23. Mainardes, R. M.; Evangelista, R. C. *Int. J. Pharm* **2005**, *290*(1-2), 137–144.

24. Yadav, K. S.; Sawant, K. K. *AAPS Pharm Sci Tech* **2010**, 11(3), 1456–1465.

25. Lince, F.; Marchisio, D. L.; Barresi, A. *A. J. Colloid Interface Sci*. **2008**, 322(2), 505–515.

26. Huang, W.; Zhang, C. *Biotechnology Journal* **2017**, 13(1), 1700203.

27. Jeon, H.-J.; Jeong, Y.-I.; Jang, M.-K.; Park, Y.-H.; Nah, J.-W. *Int. J. Pharm* **2000**, 207(1-2), 99–108.

28. Fessi, H.; Puisieux, F.; Devissaguet, J.; Ammoury, N.; Benita, S. *Int. J. Pharm*. **1989**, 55(1).

29. Cernosek, Z.; Holubova, J.; Cernoskova, E. Optoelectron. *Adv. Mat*. **2007**. 1. 277-280.

30. Rahmani, S.; Ashraf, S.; Hartmann, R.; Dishman, A. F.; Zyuzin, M. V.; Yu, C. K. J.; Parak, W. J.; Lahann, J. *Bioeng Transl Med* **2016**, 1(1), 82–93.

31. Luedtke, W. D.; Landman, U.; Chiu, Y.-H.; Levandier, D. J.; Dressler, R. A.; Sok, S.; Gordon, M. S. *J. Phys. Chem*. A A **2008**, 112(40), 9628–9649.

32. Furtmann, B.; Tang, J.; Kramer, S.; Eickner, T.; Luderer, F.; Fricker, G.; Gomez, A.; Heemskerk, B.; Jähn, P. S. *J. Pharm. Sci*. **2017**, 106(11), 3316–3327.

33. Bala, I.; Hariharan, S.; Kumar, M. R. *Crit Rev Ther Drug Carrier Syst* **2004**, 21(5), 387–422.

34. Rawat, A.; Burgess, D. J. Int. J. Pharm 2011, 415(1-2), 164–168.

REFERENCES

(Continued)

35. Mostafa, D.; El-Alim, S. A.; Kassem, A. *Nanotechnology Applications in Food* **2017**, 107–127.

36. TA INSTRUMENTS support page, http://www.tainstruments.com/pdf/literature/TA081.pdf (accessed April 26, 2019)

37. Colzani, B.; Speranza, G.; Dorati, R.; Conti, B.; Modena, T.; Bruni, G.; Zagato, E.; Vermeulen, L.; Dakwar, G. R.; Braeckmans, K.; Genta, I. *Int. J. Pharm* **2016**, 511(2), 1112–1123.

38. Rutkowski, S.; Si, T.; Gai, M.; Frueh, J.; He, Q. *RSC Advances* **2018**, *8*(43), 24243–24249.